信号通路分析辅助的功能蛋白组学研究策略

Pathway Analysis-assisted Research Strategy in Functional Proteomics

王通

暨南大学生命与健康工程研究院

Challenges in Proteomic Data Mining

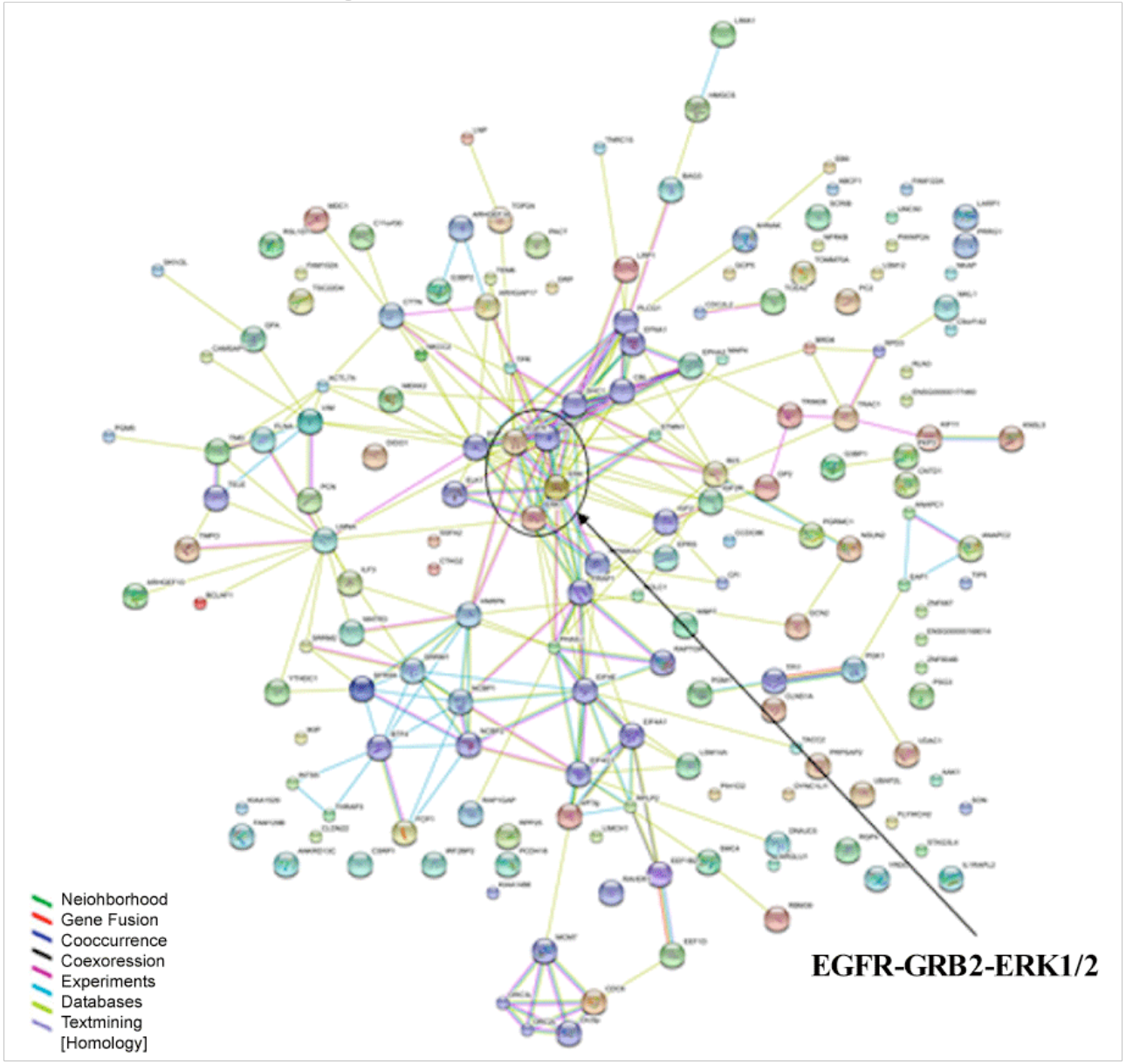

(Yan et al, 2010)

Major requirements for functional proteomic research strategy

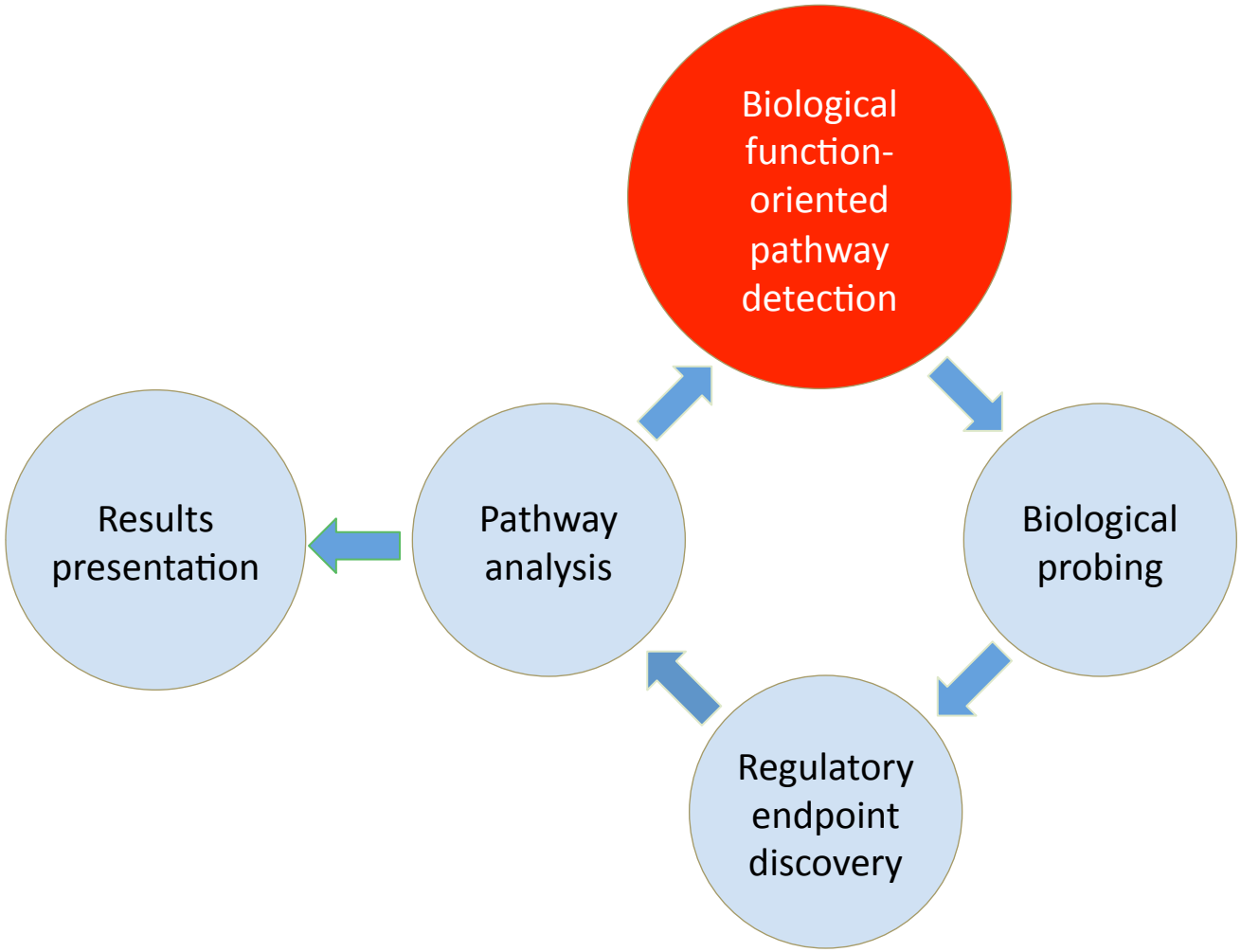

Scientific questions mentioned in this talk

- HIV associated neurodegenerative disorders (HAND)
- HIV associated malignancy (HAM)
- Infection and cancer

NIH NeuroAIDS projects Summary by Fiscal Year

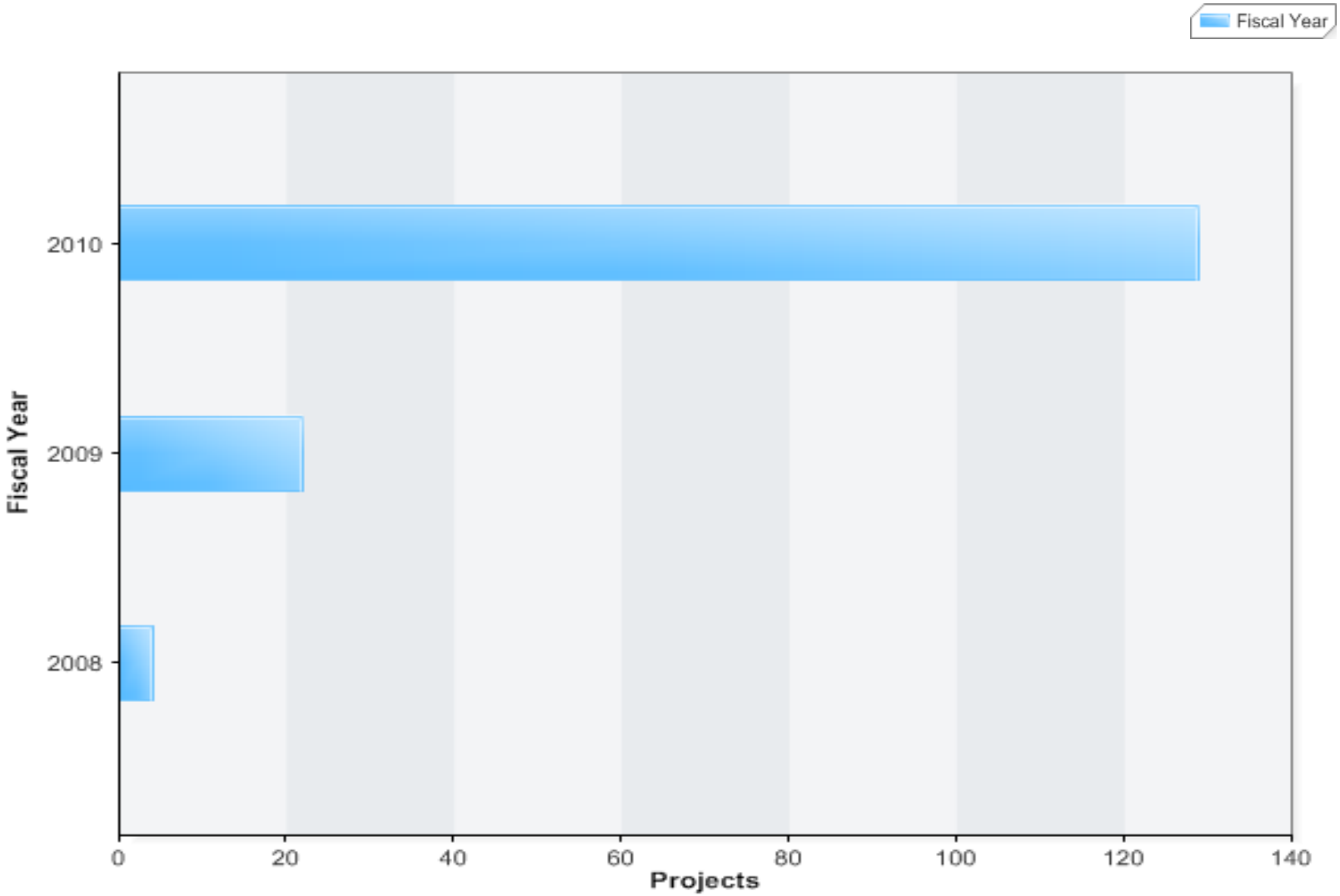

NIH funding Summary by Fiscal Year - HIV associated malignancy

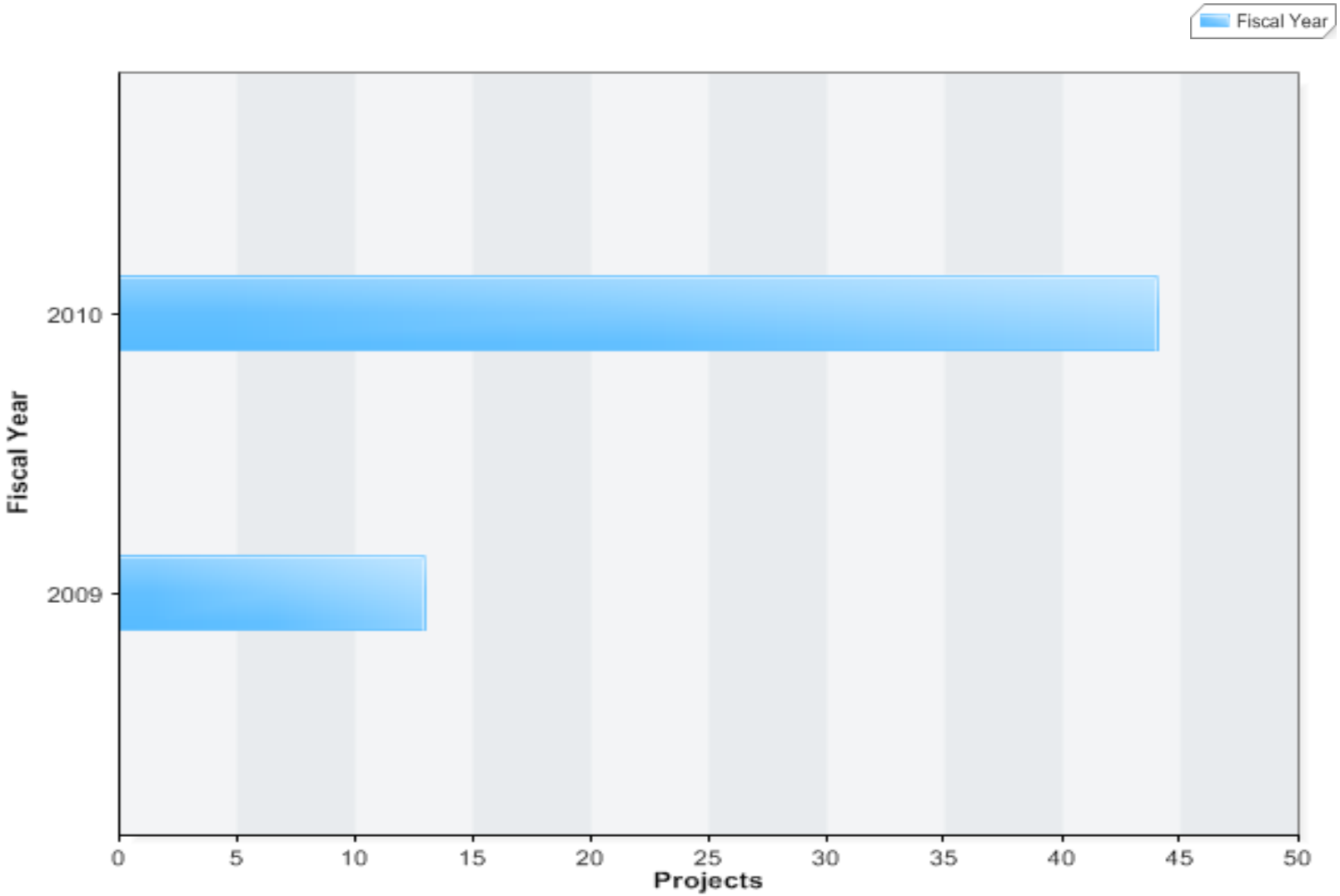

HIV Associated Neurodegeneration

- 40-70% HIV infected patients show HIV associated neurodegenerative disorders (HAND).
- AIDS dementia complex (ADC) is also known as HIV dementia, HIV encephalopathy, HIV-associated dementia (HAD).
- Prevalence is between 10-24% in Western countries.
- It is sometimes seen as the first sign of the onset of AIDS.
- Central nervous system is a reservoir of HIV-1 infection

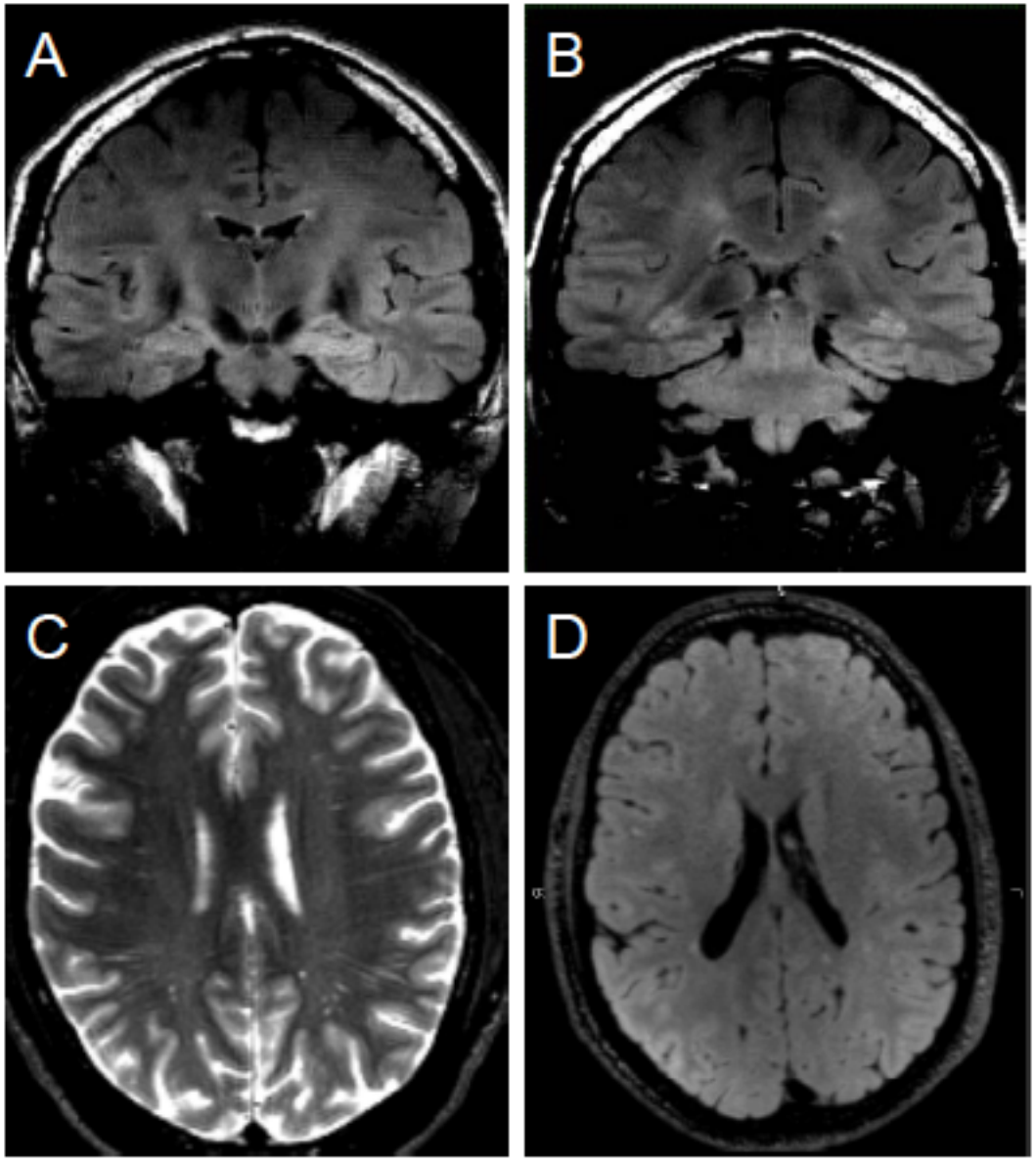

(Ho et al, 2010, CROI)

White matter lesions were the predominant abnormality detected in primary HIV infection (PHI) as early as 90 days post infection.

Question to be answered:

How do HIV virions enter CNS and cause neuronal damage?

Immune Activation and neuroAIDS

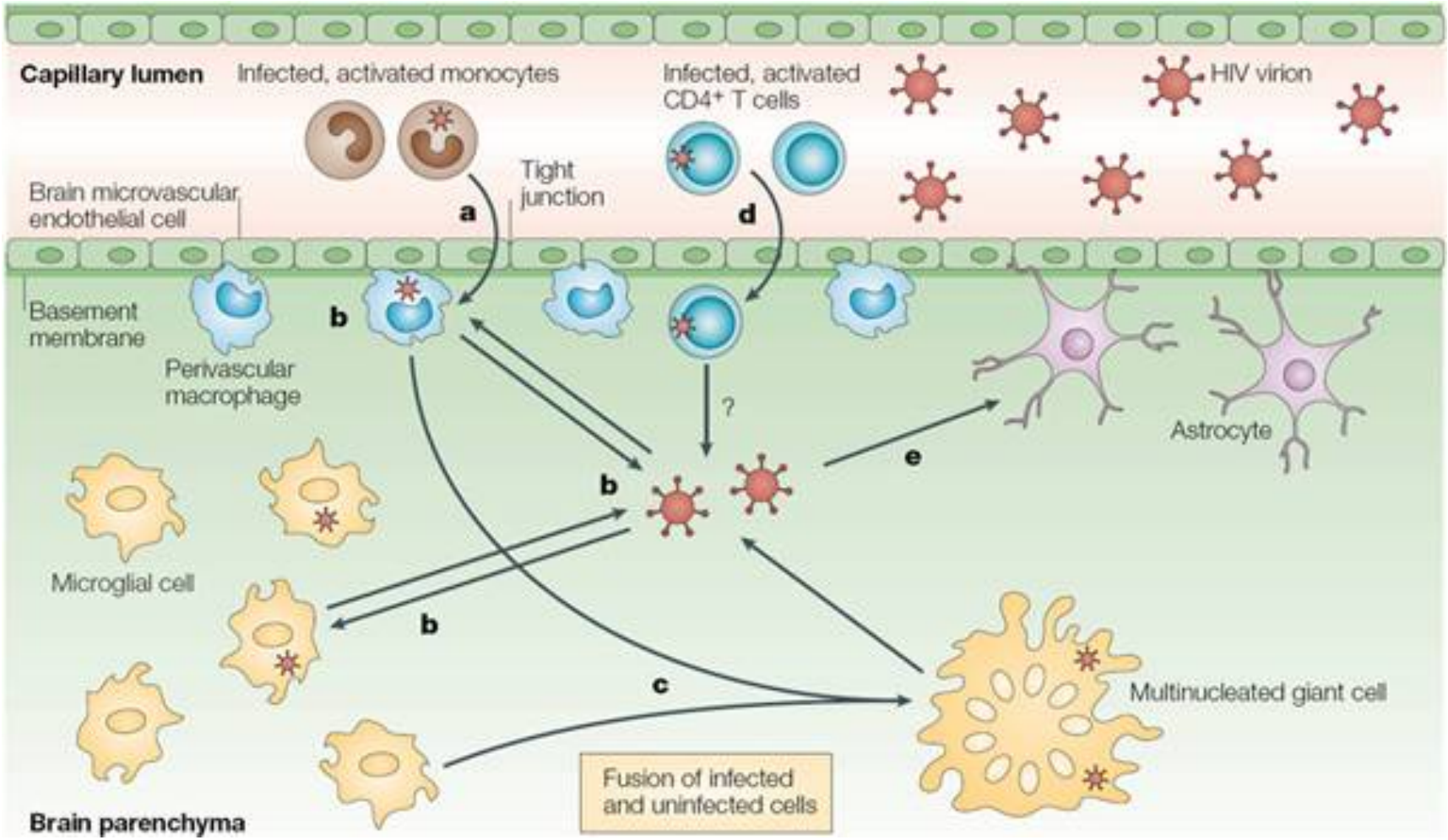

(Gonzalez-Scarano, 2005)

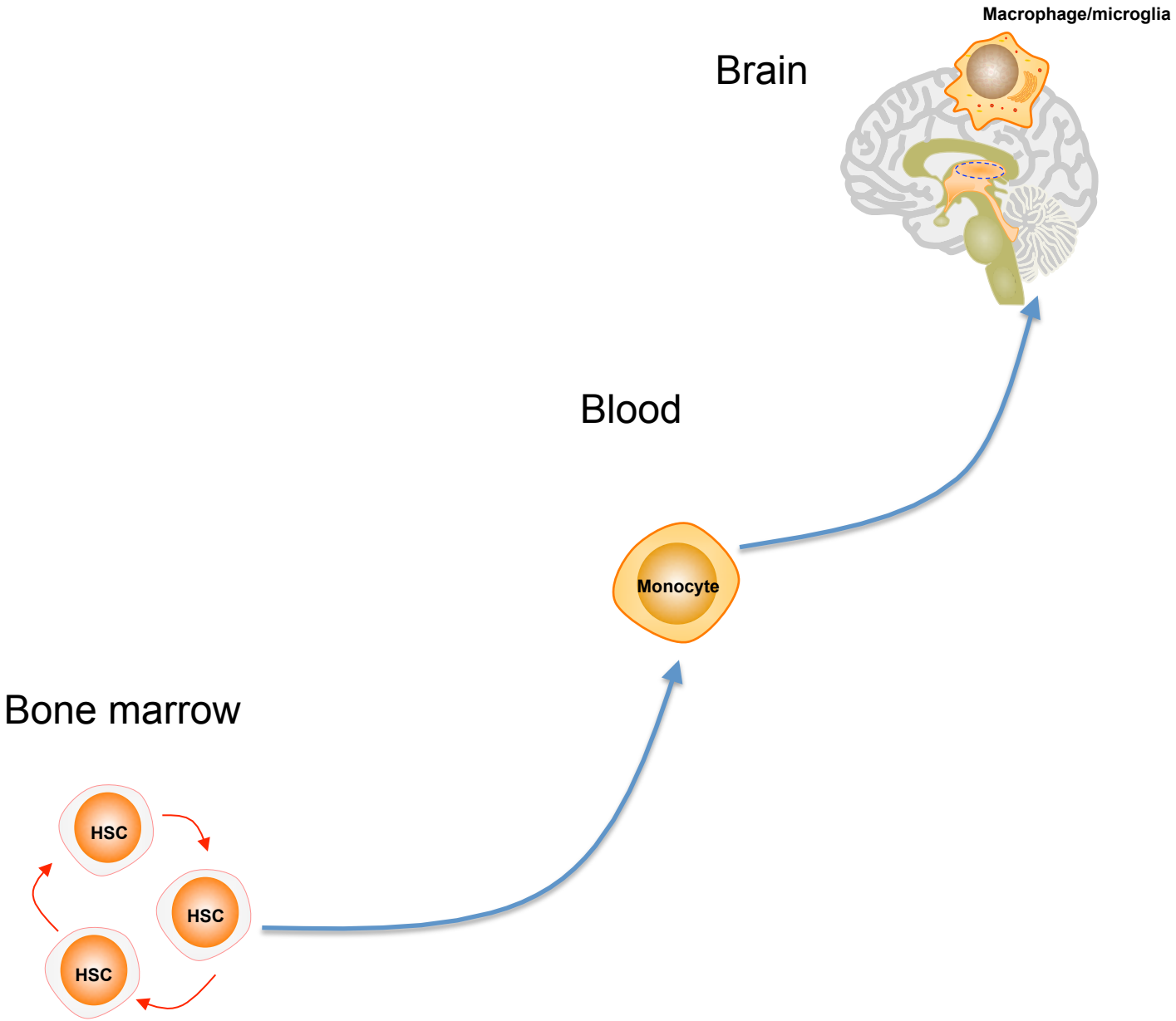
Macrophage/microglia
Brain
Blood
Monocyte
Bone marrow
HSC
HSC
HSC

Brain

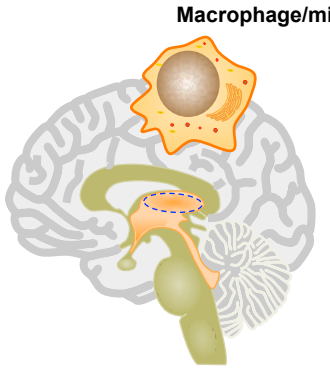

1. Astrocytes contain HIV-1 associated neurotoxicity (Wang et al, 2008a).
2. Astrocytes inhibit HIV-1 maturation in microglia (Wang et al, 2008b).

Latency

Rapid progression

Progression	Acute/early stage	Late stage
Central Nervous System		
GALT		

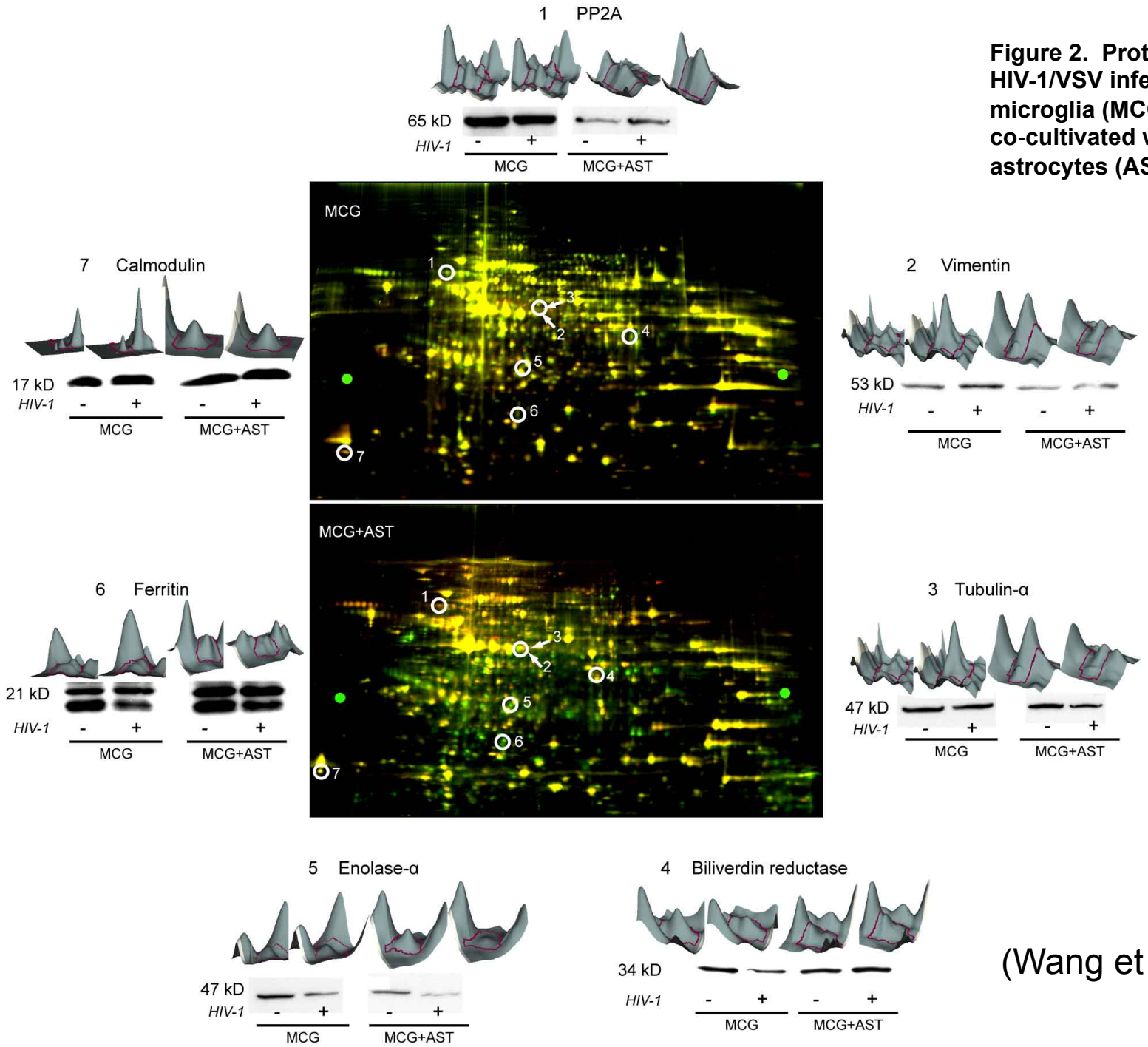

Figure 2. Proteome of HIV-1/VSV infected microglia (MCG) and MCG co-cultivated with astrocytes (AST).

(Wang et al, 2008a)

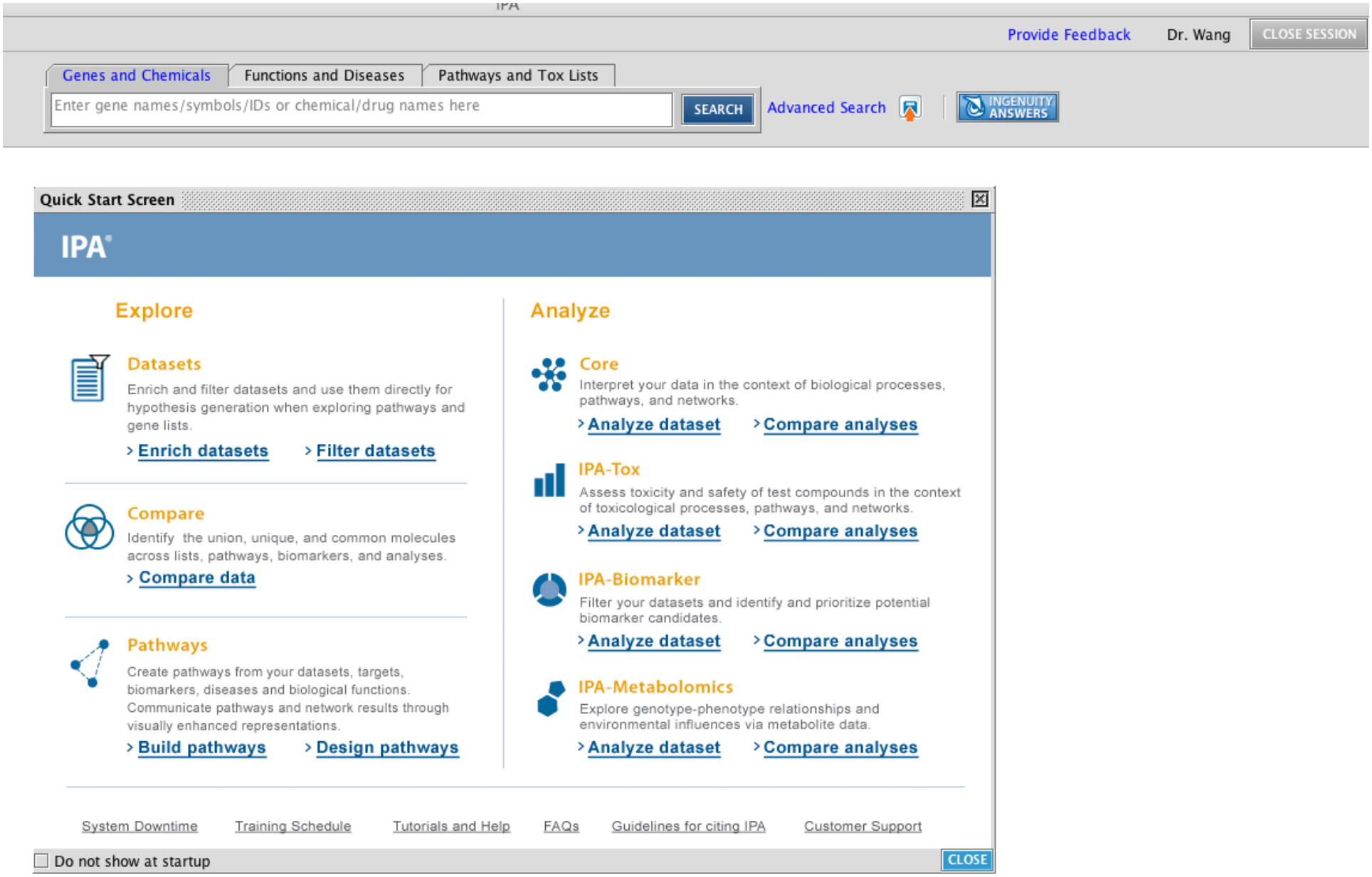

Ingenuity Pathway Analysis (IPA)

Determining Significance of Your Data to IPA Annotations

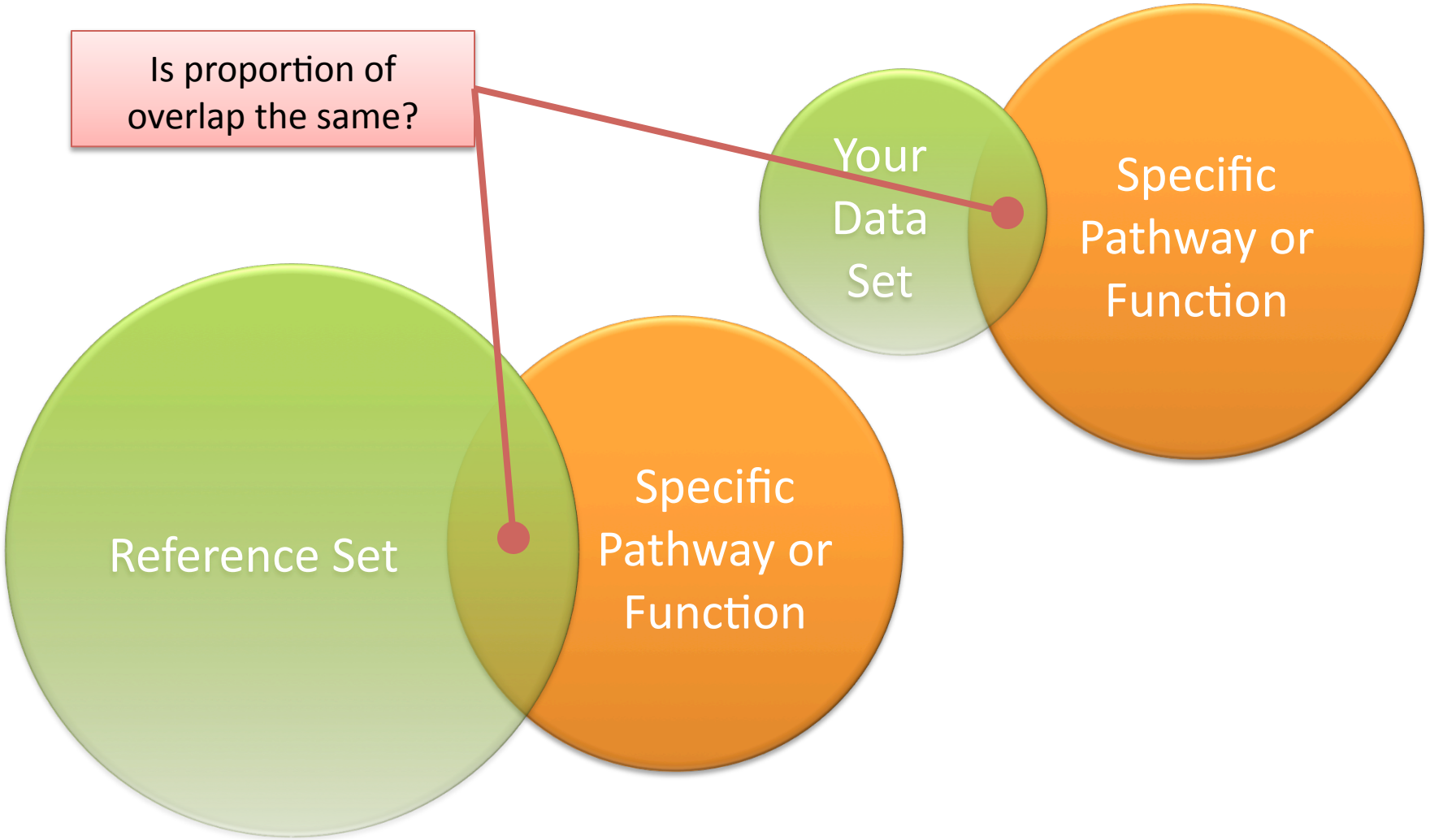

(Adapted from IPA training material with permission)

How the Fisher's Exact Test is Calculated

- The null hypothesis: The overlap (association) between the dataset and the function/pathway is due to chance. In other words, they are independent of each other.
- If the proportions mapping to a function or pathway are similar between the sample and the reference, there is not likely to be a biological effect

(Adapted from IPA training material with permission)

Significance Calculations

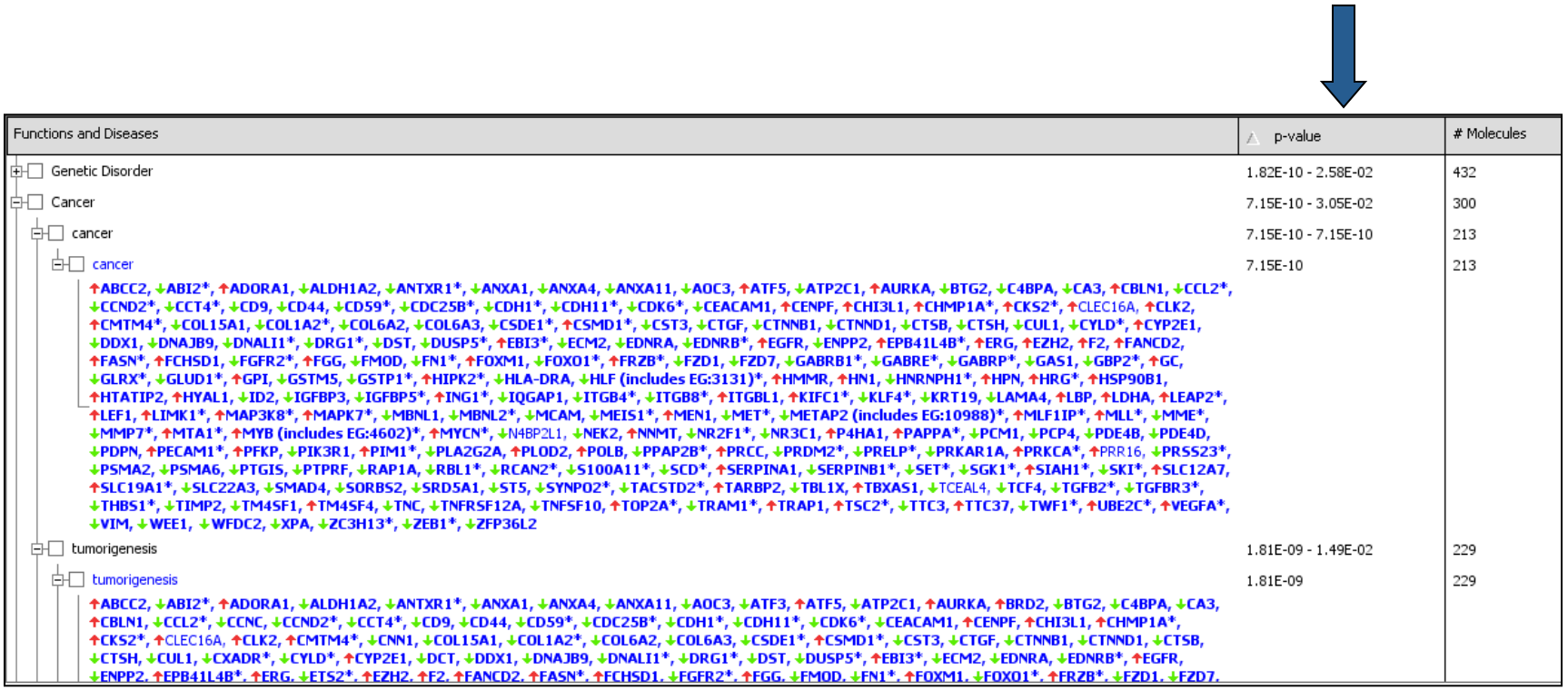

Functions and Diseases	p-value	# Molecules
Genetic Disorder	1.82E-10 - 2.58E-02	432
Cancer	7.15E-10 - 3.05E-02	300
cancer	7.15E-10 - 7.15E-10	213
cancer	7.15E-10	213
↑ABCC2, ↓ABI2*, ↑ADORA1, ↓ALDH1A2, ↓ANTXR1*, ↓ANXA1, ↓ANXA4, ↓ANXA11, ↓AOC3, ↑ATF5, ↓ATP2C1, ↑AURKA, ↓BTG2, ↓C4BPA, ↓CA3, ↑CBLN1, ↓CCL2*, ↓CCND2*, ↓CCT4*, ↓CD9, ↓CD44, ↓CD59*, ↓CDC25B*, ↓CDH1*, ↓CDH11*, ↓CDK6*, ↓CEACAM1, ↑CENPF, ↑CHI3L1, ↑CHMP1A*, ↑CKS2*, ↑CLEC16A, ↑CLK2, ↑CMTM4*, ↓COL15A1, ↓COL1A2*, ↓COL6A2, ↓COL6A3, ↓CSDE1*, ↑CSMD1*, ↓CST3, ↓CTGF, ↓CTNNB1, ↓CTNND1, ↓CTSB, ↓CTSH, ↓CUL1, ↓CYLD*, ↑CYP2E1, ↓DDX1, ↓DNAJB9, ↓DNALI1*, ↓DRG1*, ↓DST, ↓DUSP5*, ↑EBI3*, ↓ECM2, ↓EDNRA, ↓EDNRB*, ↑EGFR, ↓ENPP2, ↑EPB41L4B*, ↑ERG, ↑EZH2, ↑F2, ↑FANCD2, ↑FASN*, ↑FCHSD1, ↓FGFR2*, ↑FGG, ↓FMOD, ↓FN1*, ↑FOXM1, ↓FOXO1*, ↑FRZB*, ↓FZD1, ↓FZD7, ↓GABRB1*, ↓GABRE*, ↓GABRP*, ↓GAS1, ↓GBP2*, ↑GC, ↓GLRX*, ↓GLUD1*, ↑GPI, ↓GSTM5, ↓GSTP1*, ↑HIPK2*, ↓HLA-DRA, ↓HLF (includes EG:3131)*, ↑HMMR, ↑HN1, ↓HNRNPH1*, ↑HPN, ↑HRG*, ↑HSP90B1, ↑HTATIP2, ↑HYAL1, ↓ID2, ↓IGFBP3, ↓IGFBP5*, ↑ING1*, ↓IQGAP1, ↓ITGB4*, ↓ITGB8*, ↑ITGBL1, ↑KIFC1*, ↓KLF4*, ↓KRT19, ↓LAMA4, ↑LBP, ↑LDHA, ↑LEAP2*, ↑LEF1, ↑LIMK1*, ↑MAP3K8*, ↑MAPK7*, ↓MBNL1, ↓MBNL2*, ↓MCAM, ↓MEIS1*, ↑MEN1, ↓MET*, ↓METAP2 (includes EG:10988)*, ↑MLF1IP*, ↑MLL*, ↓MME*, ↓MMP7*, ↑MTA1*, ↑MYB (includes EG:4602)*, ↑MYCN*, ↓N4BP2L1, ↓NEK2, ↑NNMT, ↓NR2F1*, ↓NR3C1, ↑P4HA1, ↑PAPPA*, ↓PCM1, ↓PCP4, ↓PDE4B, ↓PDE4D, ↓PDPN, ↑PECAM1*, ↑PFKP, ↓PIK3R1, ↑PIM1*, ↓PLA2G2A, ↑PLOD2, ↑POLB, ↓PPAP2B*, ↑PRCC, ↓PRDM2*, ↓PRELP*, ↓PRKAR1A, ↑PRKCA*, ↑PRR16, ↓PRSS23*, ↓PSMA2, ↓PSMA6, ↓PTGIS, ↓PTPRF, ↓RAP1A, ↓RBL1*, ↓RCAN2*, ↓S100A11*, ↓SCD*, ↑SERPINA1, ↓SERPINB1*, ↓SET*, ↓SGK1*, ↑SIAH1*, ↓SKI*, ↑SLC12A7, ↑SLC19A1*, ↓SLC22A3, ↓SMAD4, ↓SORBS2, ↓SRD5A1, ↓ST5, ↓SYNPO2*, ↓TACSTD2*, ↑TARBP2, ↓TBL1X, ↑TBXAS1, ↓TCEAL4, ↓TCF4, ↓TGFB2*, ↓TGFBR3*, ↓THBS1*, ↓TIMP2, ↓TM4SF1, ↑TM4SF4, ↓TNC, ↓TNFRSF12A, ↓TNFSF10, ↑TOP2A*, ↓TRAM1*, ↑TRAP1, ↑TSC2*, ↓TTC3, ↑TTC37, ↓TWF1*, ↑UBE2C*, ↑VEGFA*, ↓VIM, ↓WEE1, ↓WFDC2, ↓XPA, ↓ZC3H13*, ↓ZEB1*, ↓ZFP36L2		
tumorigenesis	1.81E-09 - 1.49E-02	229
tumorigenesis	1.81E-09	229
↑ABCC2, ↓ABI2*, ↑ADORA1, ↓ALDH1A2, ↓ANTXR1*, ↓ANXA1, ↓ANXA4, ↓ANXA11, ↓AOC3, ↓ATF3, ↑ATF5, ↓ATP2C1, ↑AURKA, ↑BRD2, ↓BTG2, ↓C4BPA, ↓CA3, ↑CBLN1, ↓CCL2*, ↓CCNC, ↓CCND2*, ↓CCT4*, ↓CD9, ↓CD44, ↓CD59*, ↓CDC25B*, ↓CDH1*, ↓CDH11*, ↓CDK6*, ↓CEACAM1, ↑CENPF, ↑CHI3L1, ↑CHMP1A*, ↑CKS2*, ↑CLEC16A, ↑CLK2, ↑CMTM4*, ↓CNN1, ↓COL15A1, ↓COL1A2*, ↓COL6A2, ↓COL6A3, ↓CSDE1*, ↑CSMD1*, ↓CST3, ↓CTGF, ↓CTNNB1, ↓CTNND1, ↓CTSB, ↓CTSH, ↓CUL1, ↓CXADR*, ↓CYLD*, ↑CYP2E1, ↓DCT, ↓DDX1, ↓DNAJB9, ↓DNALI1*, ↓DRG1*, ↓DST, ↓DUSP5*, ↑EBI3*, ↓ECM2, ↓EDNRA, ↓EDNRB*, ↑EGFR, ↓ENPP2, ↑EPB41L4B*, ↑ERG, ↓ETS2*, ↑EZH2, ↑F2, ↑FANCD2, ↑FASN*, ↑FCHSD1, ↓FGFR2*, ↑FGG, ↓FMOD, ↓FN1*, ↑FOXM1, ↓FOXO1*, ↑FRZB*, ↓FZD1, ↓FZD7,		

- Based on right-tailed Fisher's exact test
- Only those functional annotations that have a p-value of 0.05 or smaller are displayed

(Adapted from IPA training material with permission)

A

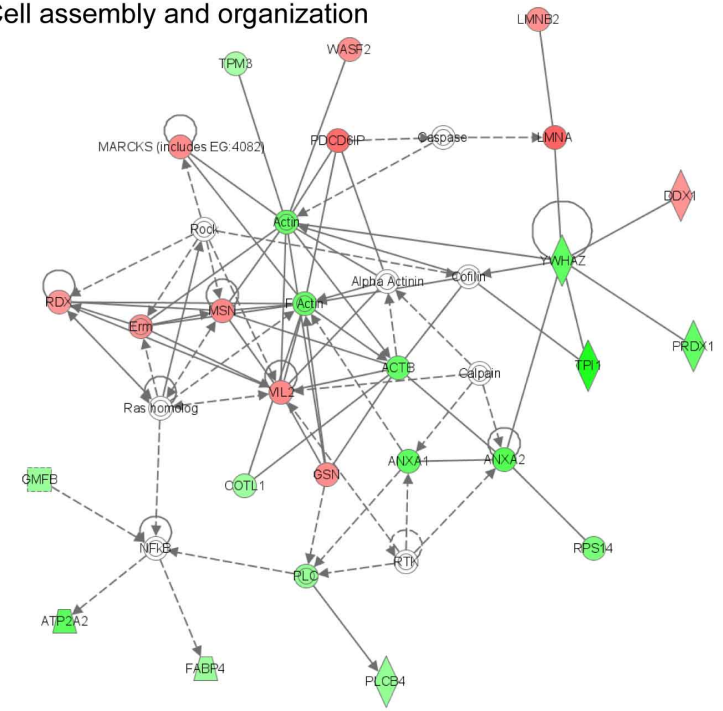

B

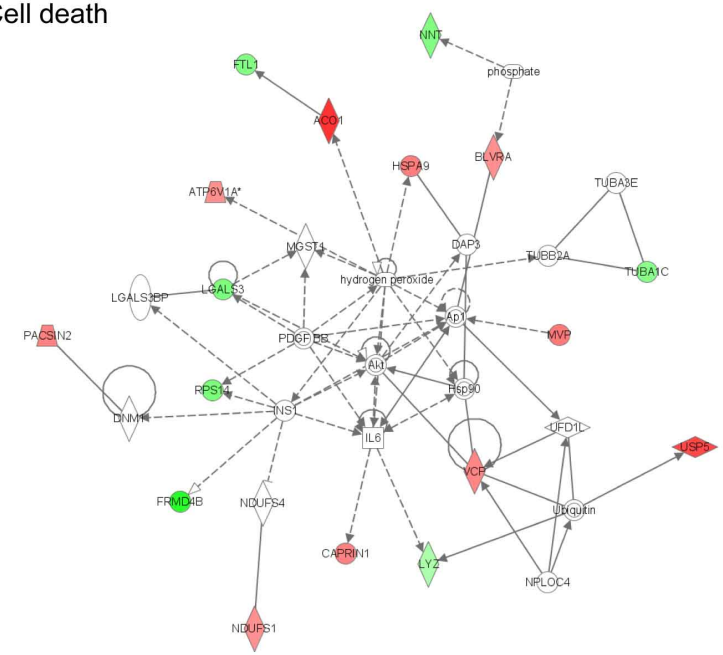

Figure 3. Ingenuity Pathway Analysis.

(Wang et al, 2008a)

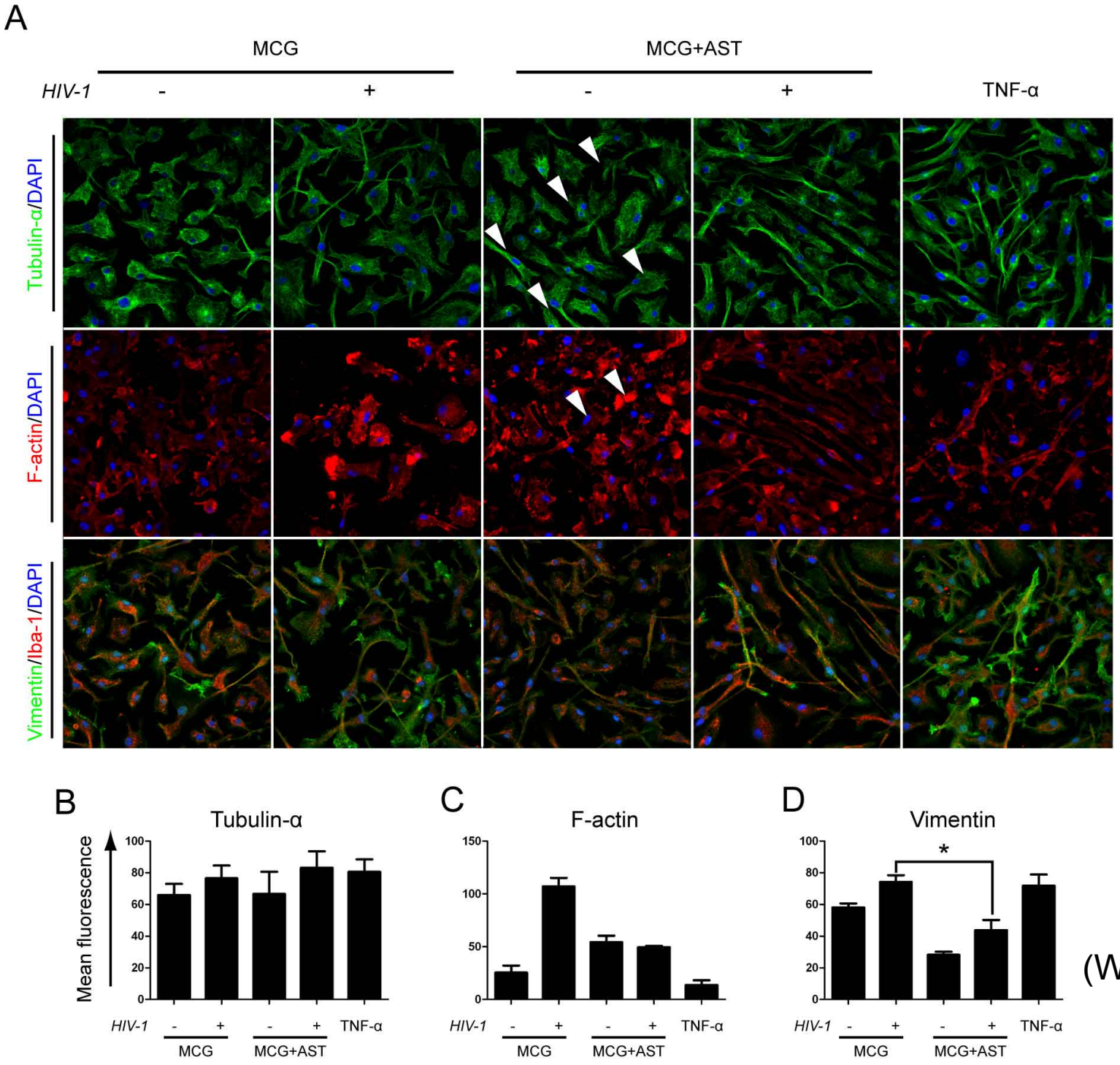

Figure 4. Immunohistochemical validation of proteomic profiling.

(Wang et al, 2008a)

Brain

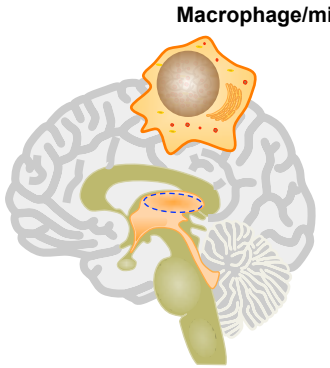

1. Astrocytes contain HIV-1 associated neurotoxicity (Wang et al, 2008a).
2. Astrocytes inhibit HIV-1 maturation in microglia (Wang et al, 2008b).
3. HIV-1 infected microglia show migratory phenotypes (Wang et al, 2008a).

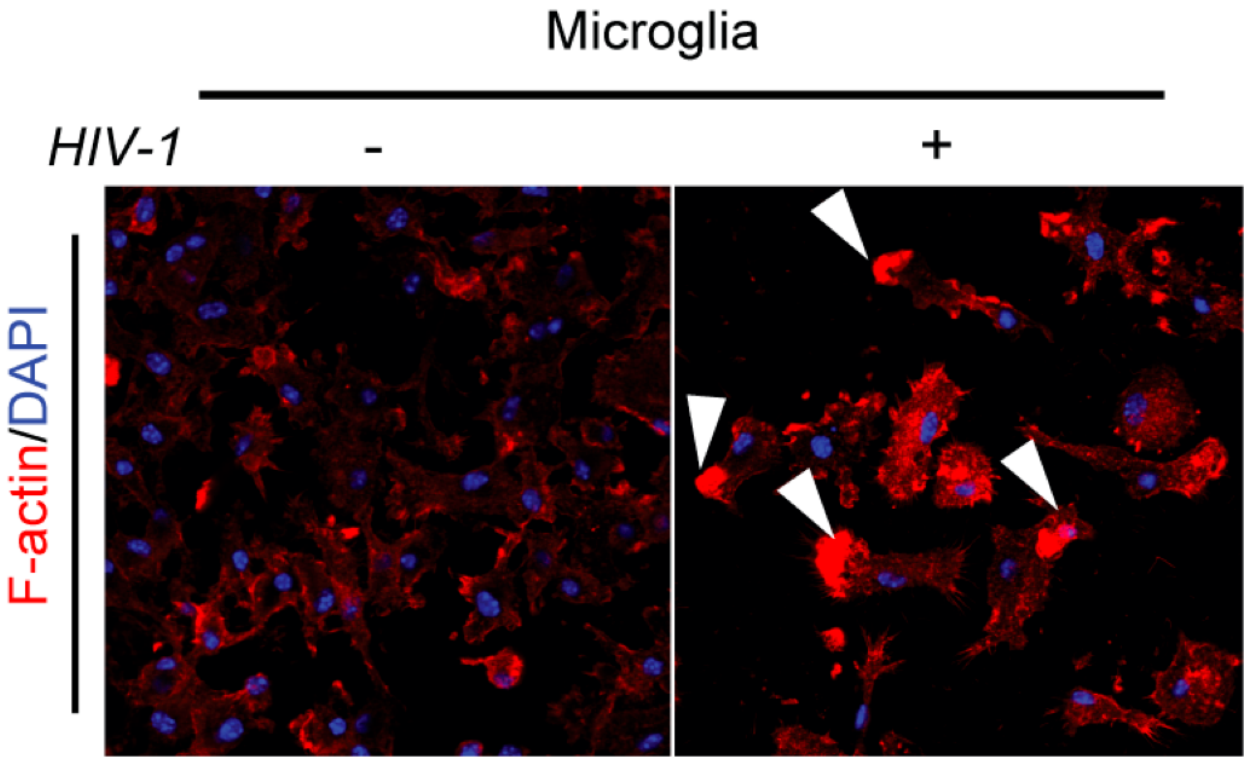

(Wang et al, 2008a)

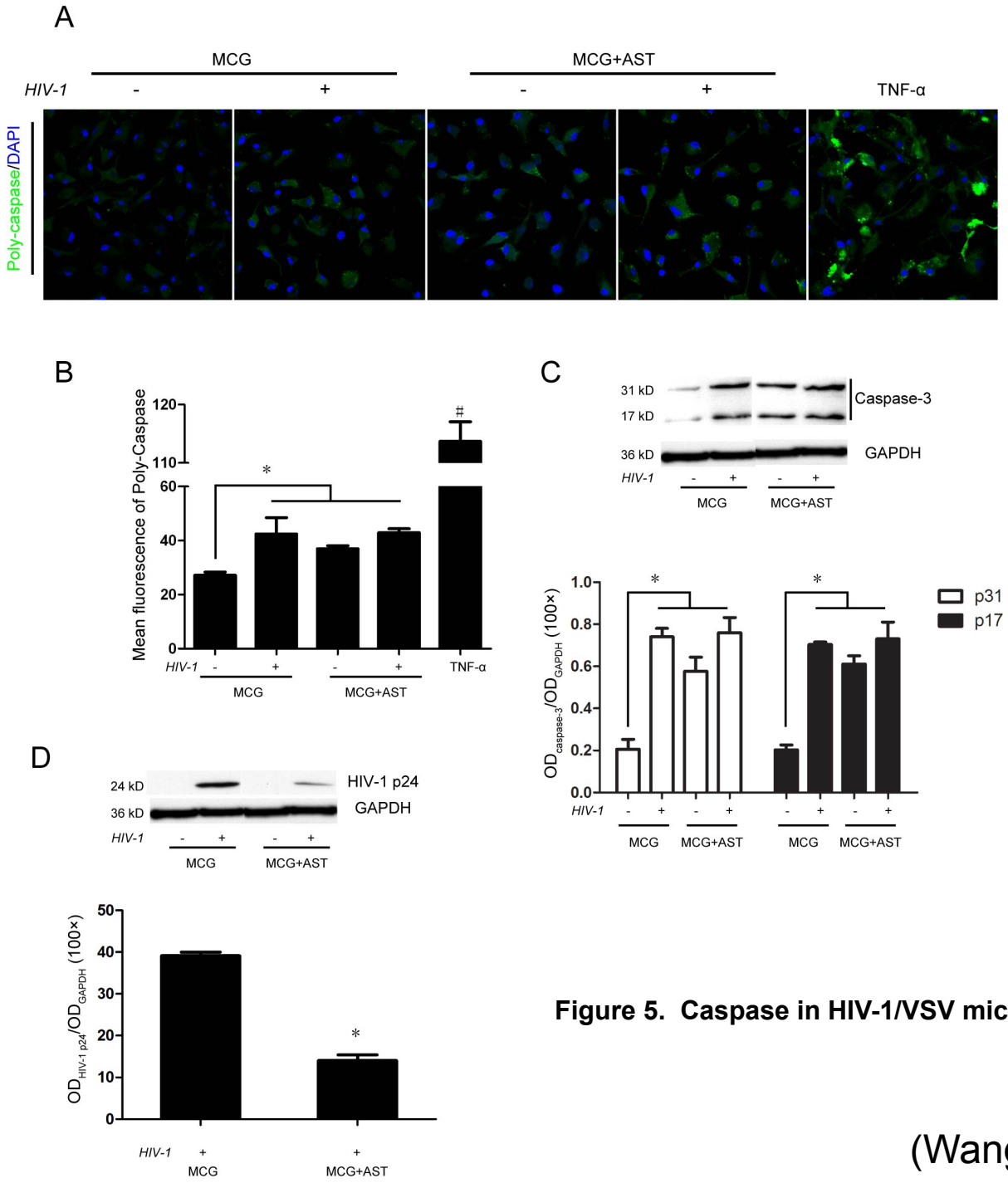

Figure 5. Caspase in HIV-1/VSV microglial infections.

(Wang et al, 2008a)

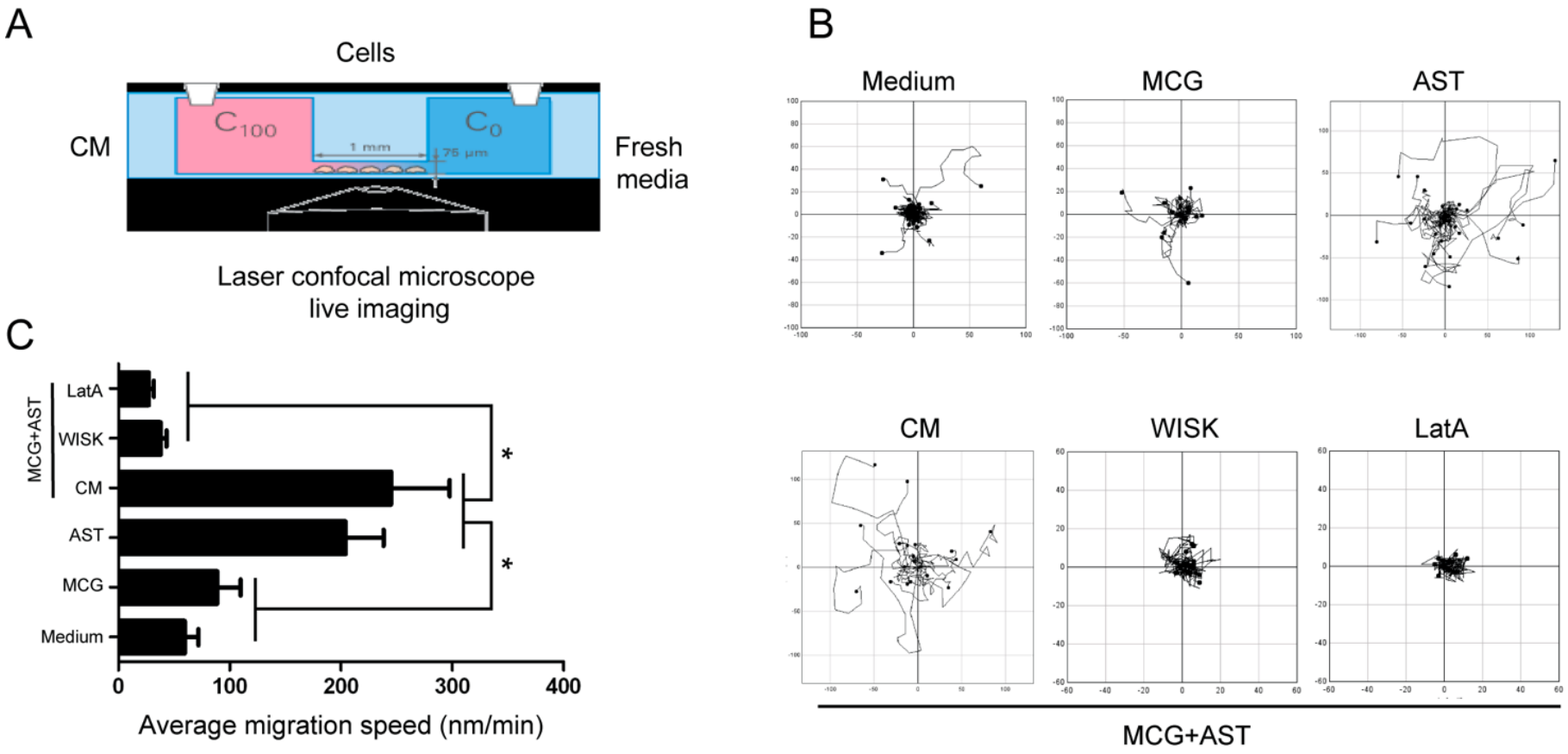

Figure 5. The mobility changes of monocyte/macrophages after exposure to microglia/astrocytes conditioned media.

(Wang et al, 2008a)

What if astrocytes become bad guys?

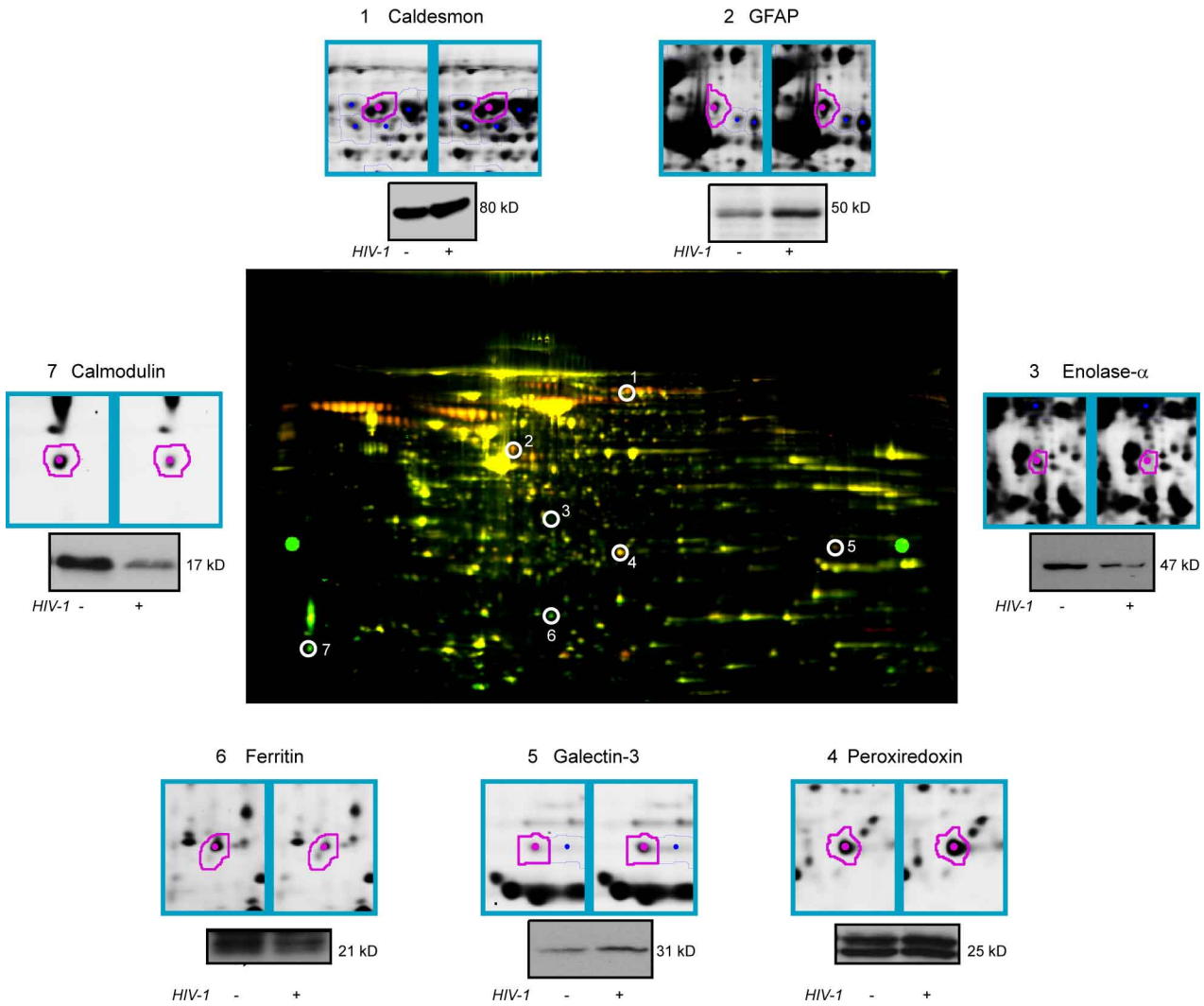

(Wang et al, 2008b)

Cell death, DNA replication, recombination and repair

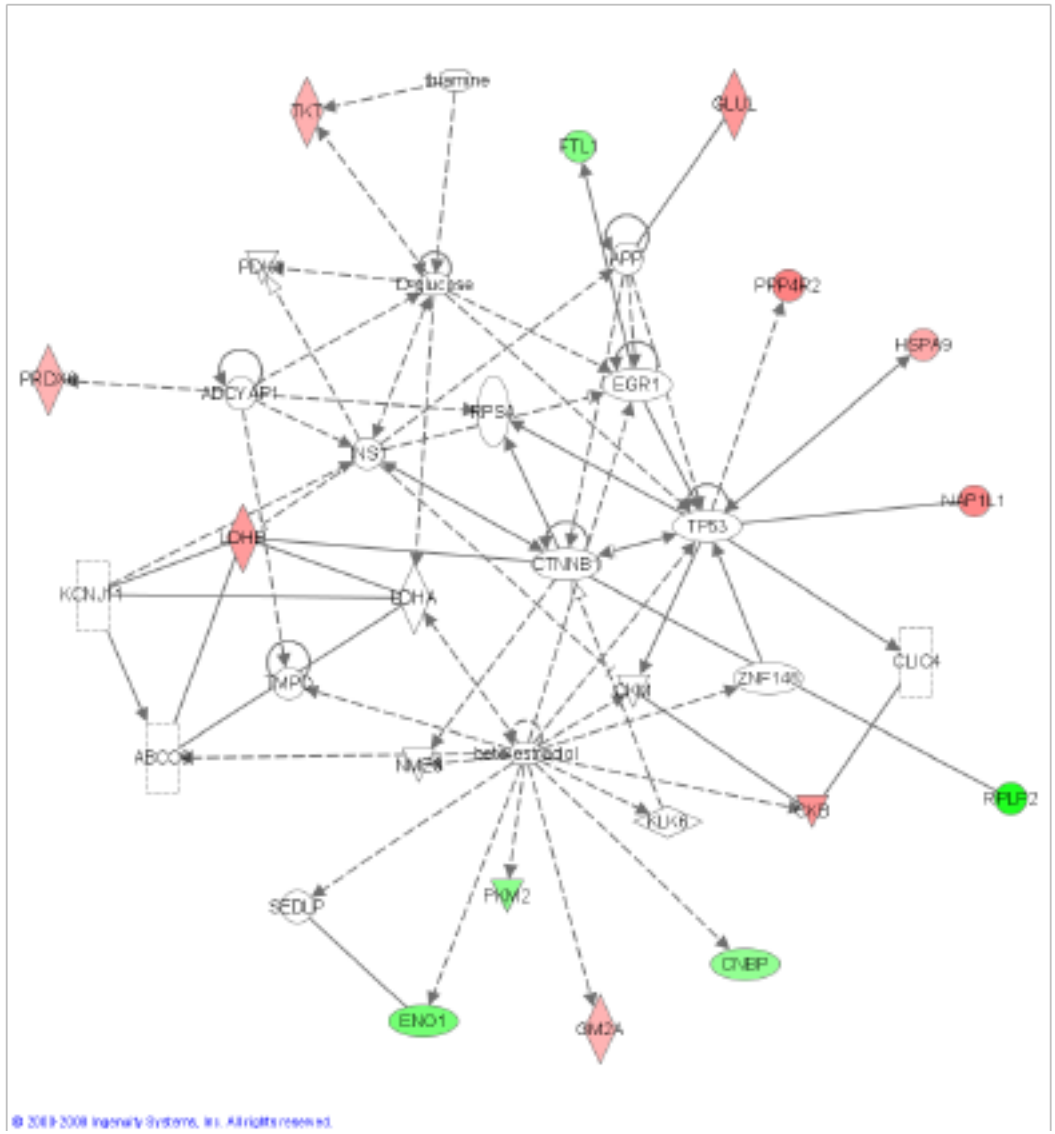

Figure 4. Ingenuity Pathway Analysis

(Wang et al, 2008b)

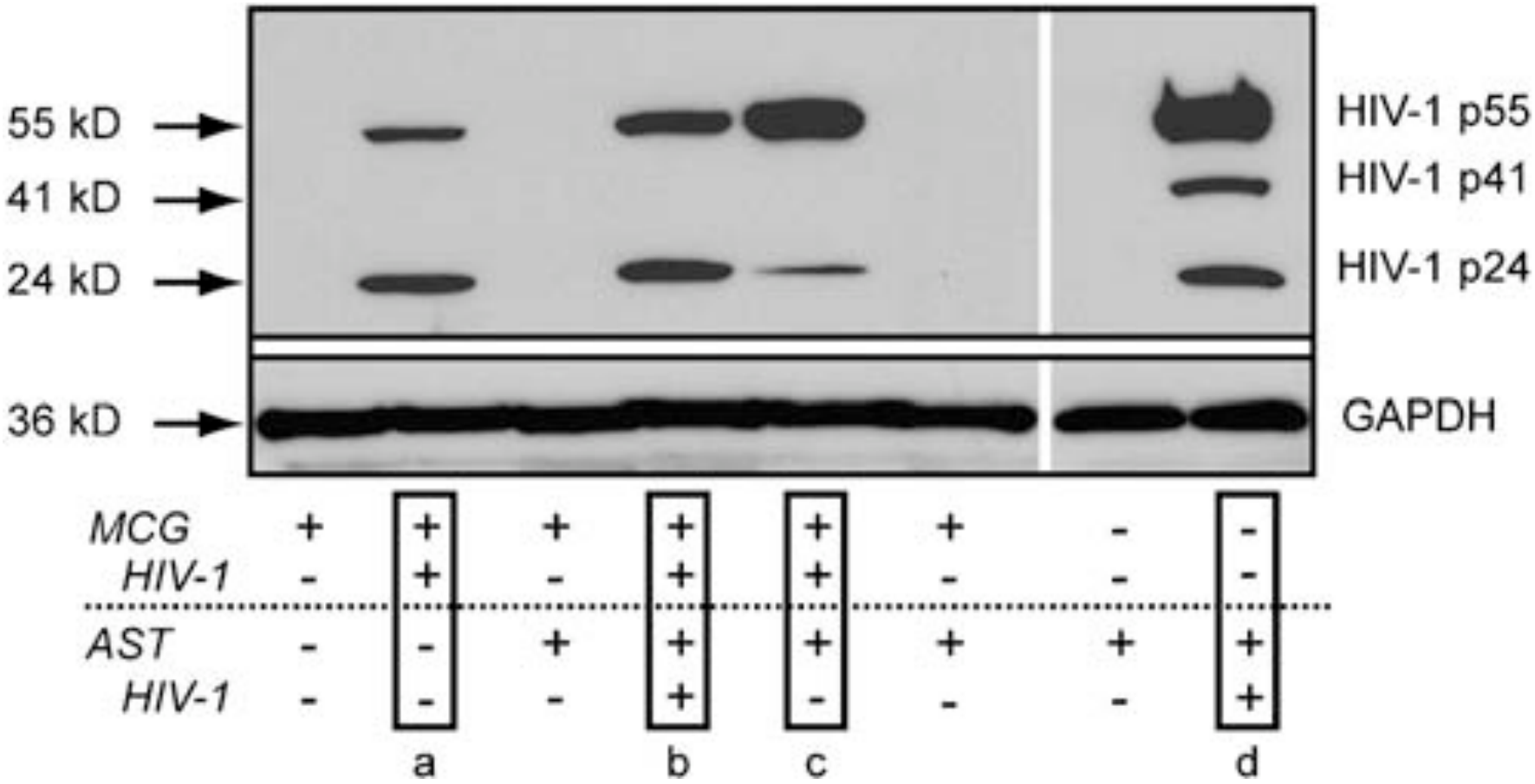

Fig. 5 HIV-1 p24 protein processing. **(Wang et al, 2008b)**

Hori, K., Burd, P.R., Kutza, J., Weih, K.A., and Clouse, K.A. Human astrocytes inhibit HIV-1 expression in monocyte-derived macrophages by secreted factors, *AIDS* **13**, 751-8 (1999). PMID: 10357373

Leone, C., Le Pavec, G., Meme, W., Porcheray, F., Samah, B., Dormont, D., and Gras, G. Characterization of human monocyte-derived microglia-like cells, *Glia* **54**, 183-92 (2006). PMID: 16807899

Brain

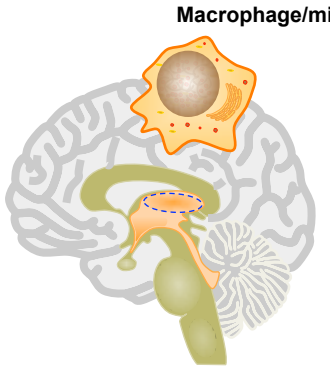

1. Astrocytes contain HIV-1 associated neurotoxicity (Wang et al, 2008a).
2. Astrocytes inhibit HIV-1 maturation in microglia (Wang et al, 2008b).
3. HIV-1 infected microglia show migratory phenotypes (Wang et al, 2008a).
4. Most HIV-1 found in brain are M-tropic (Gonzalez-Perez et al, 2010).

Session 88-Poster Abstracts
Infection and Immune Activation of CNS Compartments
Thursday, 2-4 pm; Poster Hall

Paper # 425

Compartmentalization of HIV-1 Macrophage-tropism in Brain Tissue of Patients with HIV-associated Dementia

Maria Paz Gonzalez-Perez* and P Clapham
Univ of Massachusetts Med Sch, Worcester, US

Background: Several groups have reported the presence of highly mac-tropic R5 envelopes in brain tissue of AIDS patients with neurological complications. However, these studies have investigated very few subjects and have differed in the extent of compartmentalization of macrophage-tropism between the brain and immune tissue. Here, we have investigated compartmentalization of genotypes in 225 subjects and 67 mac-tropism of envelopes amplified from brain and spleen or lymph node (LN) of 5 HAD subjects.

Methods: Envelopes were amplified from proviral and episomal DNA from single genomes present in brain and spleen or LN tissue using high fidelity DNA polymerases. Envs were cloned into the pcDNA 3.1D/V5-His-TOPO and sequenced. Env+ pseudovirions were prepared by cotransfection of env vectors with env$^-$ pNL4.3 into 293T cells and titrated on HeLa TZM-BL (CD4$^+$ CCR5$^+$ CXCR4$^+$), HIJ (CD4$^+$ CCR5$^-$ CXCR4$^+$) and on macrophages. Nucleotide sequences were aligned using Clustal X and phylogenetic analyses undertaken with MEGA v4.

Results: All envs amplified from brain tissue were R5. We observed compartmentalization of sequence and mac-tropism for 4 of 5 subjects, although for one subject only 3 *envs* were obtained from brain. For one subject, compartmentalization of genotypes was not apparent although the majority of brain *envs* were mac-tropic, while the majority of *envs* from spleen/LN were not. Envs from episomal DNA did not segregate separately from those derived from proviral DNA. Examples of closely related envs that differed markedly in mac-tropism were identified in LN and brain. No association between gp120 charge, length or number of N-linked CHO sites was observed. For one subject, envs from brain carried N283 (previously associated with mac-tropism and dementia). However, for two subjects nearly all envs from spleen/LN and brain carried N283.

Conclusions: The extent of compartmentalization of HIV-1 env genotypes and mac-tropism in the brain varied depending on subject. However, even when sequence compartmentalization was not apparent, mac-tropism segregated more clearly with a brain origin. This observation together with the identification of closely related envs that differed markedly in mac-tropism in spleen, LN and brain, strongly indicate that distinct selective pressures at these sites can modulate mac-tropism.

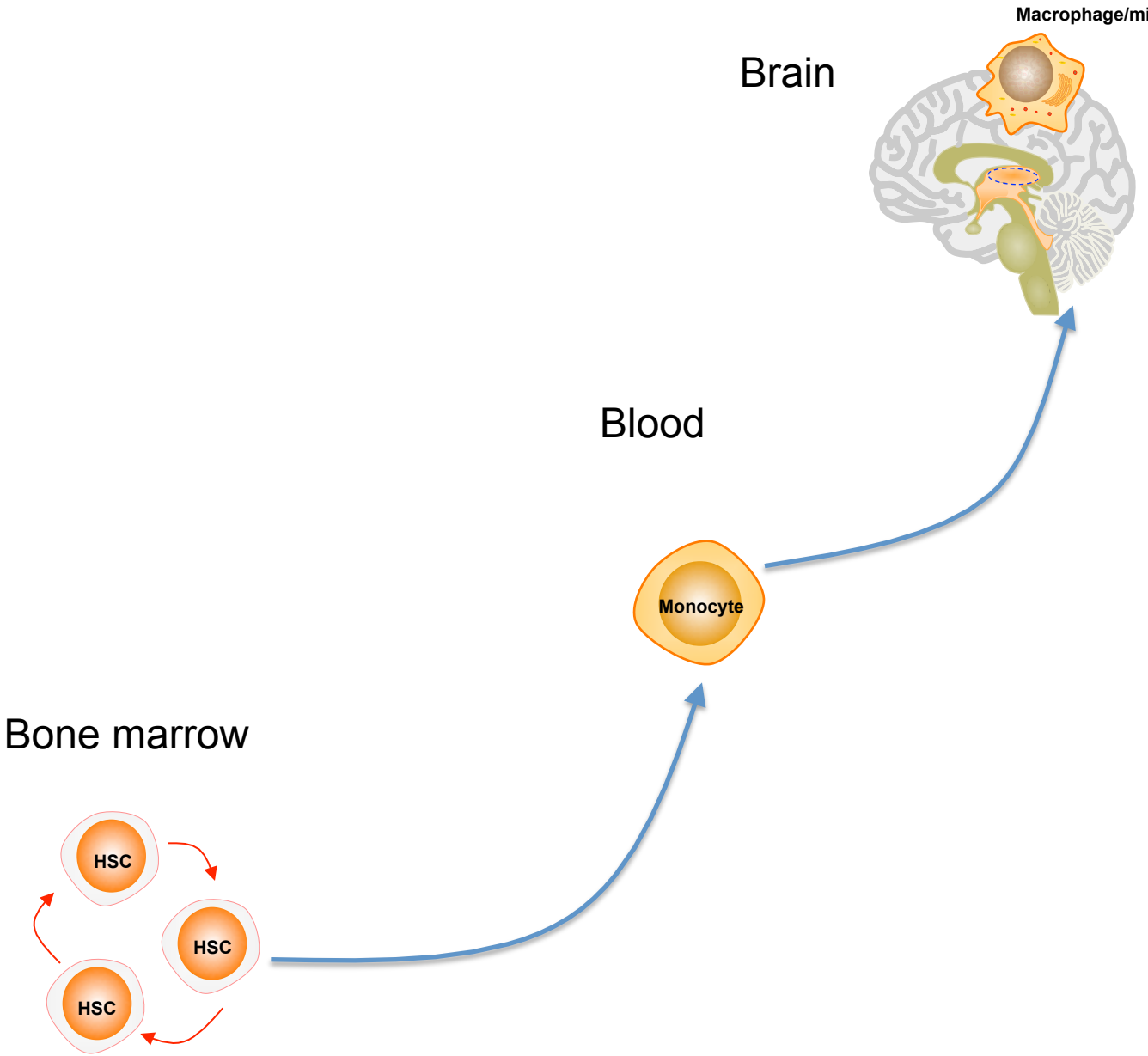

1. Astrocytes contain HIV-1 associated neurotoxicity (Wang et al, 2008a).
2. Astrocytes inhibit HIV-1 maturation in microglia (Wang et al, 2008b).
3. HIV-1 infected microglia show migratory phenotypes (Wang et al, 2008a).
4. Most HIV-1 found in brain are M-tropic (Gonzalez-Perez et al, 2010).

Blood

1. Monocytes can harbor HIV-1.
2. In all cases we studied, HIV-1 show compartmentalization between monocytes and CD4+ T cells (Zhu et al, 2002; Llewellyn et al, 2006; Fulcher et al, 2004).

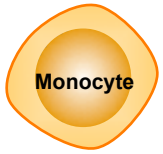

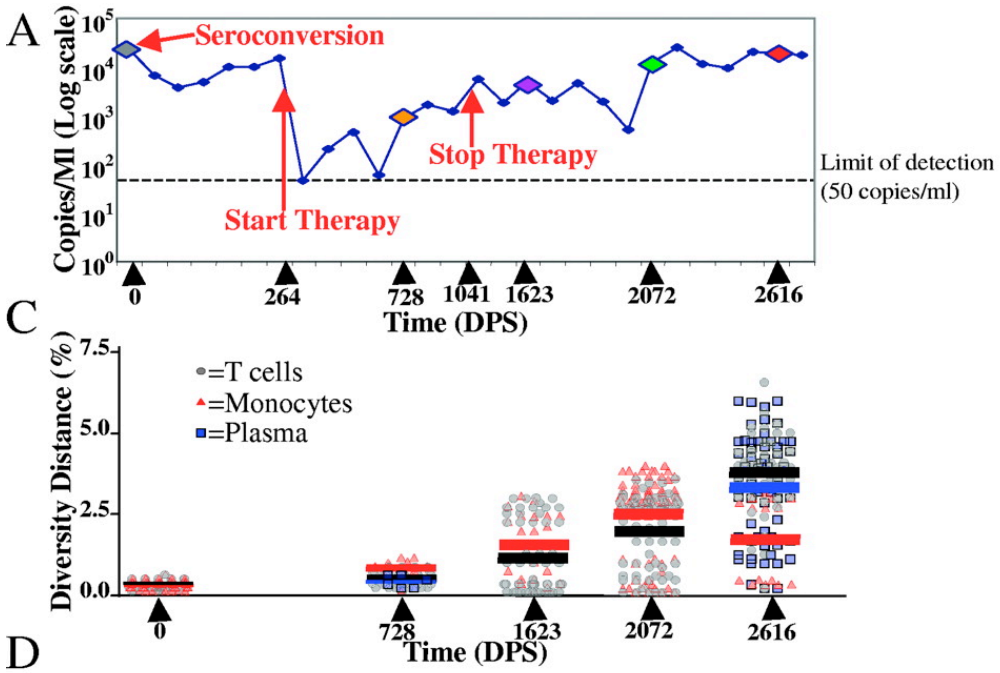

D

Diversity P-Value	T/M=0.39	T/M=**<0.001** T/PL=0.38 M/PL=**0.0083**	T/M=0.17	T/M=**0.0043**	T/M=**<0.001** T/PL=0.095 M/PL=**<0.001**
Compartm-entalization P-Value	T/M=0.233	T/M=**0.008** T/PL=**0.002** M/PL=**0.018**	T/M=0.259	T/M=0.104	T/M=**0.002** T/PL=**<0.001** M/PL=**0.001**
Viral Load	22808	909	4899	12005	19131
CD4 Count	848	954	724	1009	465
CD8 Count	552	737	609	913	587

Subject 1175

(Llewellyn et al, 2006)

Blood

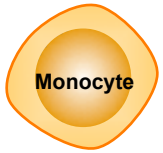

1. Monocytes can harbor HIV-1.
2. In all cases we studied, HIV-1 show compartmentalization between monocytes and CD4+ T cells (Zhu et al, 2002; Llewellyn et al, 2006; Fulcher et al, 2004).
3. Level of HIV DNA in monocytes are linked with HAND/ dementia (Valcour et al, 2010).

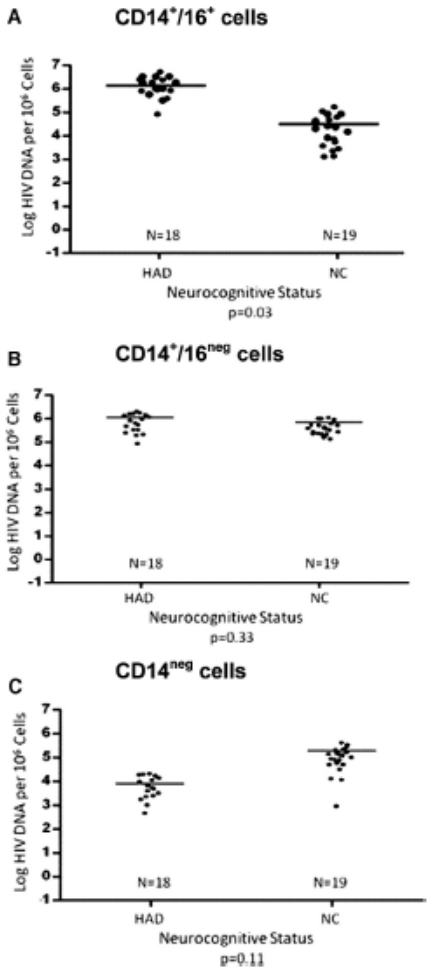

(Shiramizu et al, 2007)

Brain

Macrophage/microglia

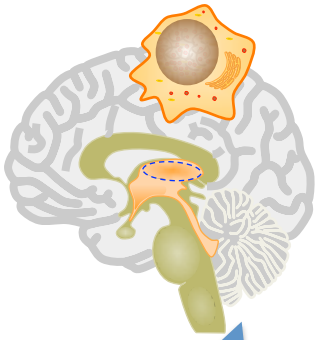

1. Astrocytes contain HIV-1 associated neurotoxicity (Wang et al, 2008a).
2. Astrocytes inhibit HIV-1 maturation in microglia (Wang et al, 2008b).
3. HIV-1 infected microglia show migratory phenotypes (Wang et al, 2008a).
4. Most HIV-1 found in brain are M-tropic (Gonzalez-Perez et al, 2010).

Blood

Monocyte

1. Monocytes can harbor HIV-1 .
2. In some cases, HIV-1 show compartmentalization between monocytes and CD4+ T cells (Fulcher et al, 2004; Llewellyn et al, 2006).
3. Level of HIV DNA in monocytes are linked with HAND/dementia (Valcour et al, 2010).

Bone marrow

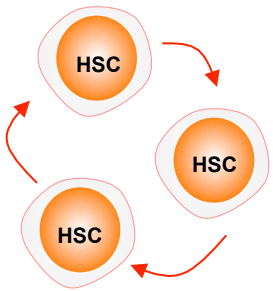

Bone marrow

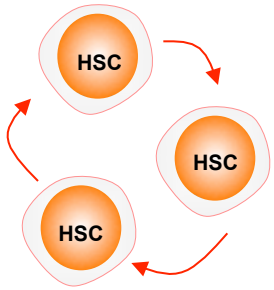

1. HIV-1 infects multipotent progenitor cells causing cell death and establishing latent cellular reservoirs (Carter et al, 2010).

Nat Med. 2010 Mar 7. [Epub ahead of print]

HIV-1 infects multipotent progenitor cells causing cell death and establishing latent cellular reservoirs.

Carter CC, Onafuwa-Nuga A, McNamara LA, Riddell J 4th, Bixby D, Savona MR, Collins KL.

[1] Graduate Program in Cellular and Molecular Biology, University of Michigan, Ann Arbor, Michigan, USA. [2] Medical Scientist Training Program, University of Michigan, Ann Arbor, Michigan, USA. [3] These authors contributed equally to this work.

HIV causes a chronic infection characterized by depletion of CD4(+) T lymphocytes and the development of opportunistic infections. Despite drugs that inhibit viral spread, HIV infection has been difficult to cure because of uncharacterized reservoirs of infected cells that are resistant to highly active antiretroviral therapy (HAART) and the immune response. Here we used CD34(+) cells from infected people as well as in vitro studies of wild-type HIV to show infection and killing of CD34(+) multipotent hematopoietic progenitor cells (HPCs). In some HPCs, we detected latent infection that stably persisted in cell culture until viral gene expression was activated by differentiation factors. A unique reporter HIV that directly detects latently infected cells in vitro confirmed the presence of distinct populations of active and latently infected HPCs. These findings have major implications for understanding HIV bone marrow pathology and the mechanisms by which HIV causes persistent infection.

PMID: 20208541 [PubMed - as supplied by publisher]

Bone marrow

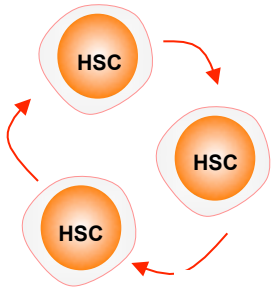

1. HIV-1 infects multipotent progenitor cells causing cell death and establishing latent cellular reservoirs (Carter et al, 2010).
2. Reconstitution of bone marrow with CCR5-disrupted HSC can control HIV-1 in vivo (Hutter et al, 2009).

The NEW ENGLAND JOURNAL of MEDICINE

BRIEF REPORT

Long-Term Control of HIV by *CCR5* Delta32/Delta32 Stem-Cell Transplantation

Gero Hütter, M.D., Daniel Nowak, M.D., Maximilian Mossner, B.S., Susanne Ganepola, M.D., Arne Müßig, M.D., Kristina Allers, Ph.D., Thomas Schneider, M.D., Ph.D., Jörg Hofmann, Ph.D., Claudia Kücherer, M.D., Olga Blau, M.D., Igor W. Blau, M.D., Wolf K. Hofmann, M.D., and Eckhard Thiel, M.D.

What is missing?

Brain

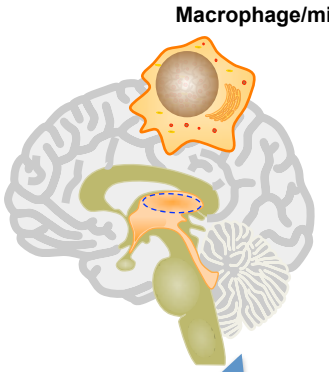

1. Astrocytes contain HIV-1 associated neurotoxicity (Wang et al, 2008a).
2. Astrocytes inhibit HIV-1 maturation in microglia (Wang et al, 2008b).
3. HIV-1 infected microglia show migratory phenotypes (Wang et al, 2008a).
4. Most HIV-1 found in brain are M-tropic (Gonzalez-Perez et al, 2010).

Blood

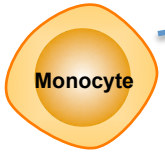

1. Monocytes can harbor HIV-1 .
2. In some cases, HIV-1 show compartmentalization between monocytes and CD4+ T cells (Fulcher et al, 2004; Llewellyn et al, 2006).
3. Level of HIV DNA in monocytes are linked with HAND/dementia (Valcour et al, 2010).

Bone marrow

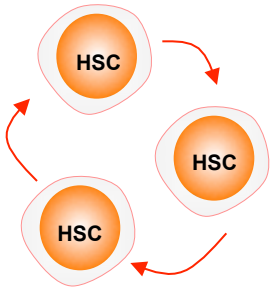

1. HIV-1 infects multipotent progenitor cells causing cell death and establishing latent cellular reservoirs (Carter et al, 2010).
2. Reconstitution of bone marrow with CCR5-disrupted HSC can control HIV-1 in vivo (Hutter et al, 2009).

HIV associated inflammation and Cancer microenvironment

Hypothesis

Unintegrated HIV DNA in macrophages can release inflammatory viral and host cell products, thus co-activating bystander normal tissue cells. This inter-cellular crosstalk generates a microenvironment that is relevant to cancer progression.

A novel cue of cancer microenvironment - Unintegrated HIV DNA in macrophages

1. Unintergrated HIV DNA persists in macrophages (Kim et al., 1989; Muesing et al., 1985; Pang et al., 1990; Pauza, Galindo, and Richman, 1990)
2. Transcription of these unintergrated HIV DNA in macrophages is long-term active (Kelly et al, 2008).

HIV associated malignancy	Can HAART reduce the incidence?
Kaposi's sarcoma	Significantly
Cervical cancer	Non-significantly
Non-Hodgkin's lymphoma (Colon cancer)	Non-significantly

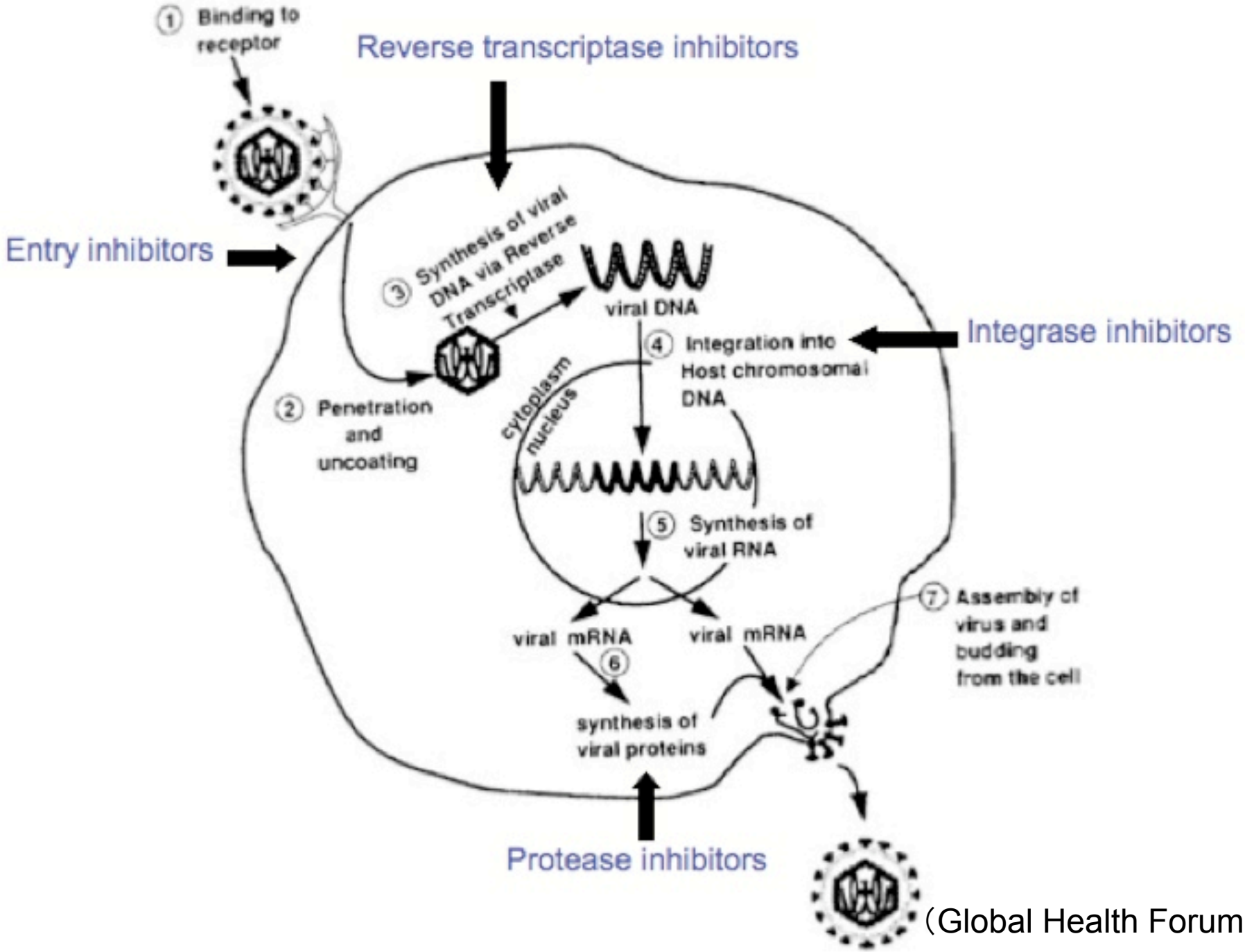

（Global Health Forum）

Several players in the game

1. HIV Viral protein R
2. HIV gp120
3. Bone marrow/monocyte derived macrophages
4. Cancer cells (such as sarcoma, cervical cancer, CNS cancer, NHL and others)
5. Other cancer-educated cells

Viral Protein R

Fig. 1 Functional Vpr expressed endogenously in C8166 cells. **a** GFP expression in mock-, rAd-vector and rAd-*vpr* infected groups. Cells with either mock or viral infections were cultured for 24 h. GFP was detected at FL1 channel in flowcytometry and data shown are representative of three independent experiments. *M1* region shows GFP positive cells. **b** Representative images of GFP expression in different groups (*scale bar* = 10 μm), followed by western blotting confirmation of HIV-1 Vpr in C8166 cells. **c** Cell cycle and cell death of C8166 cells. Cells were stained with propidium iodide and analyzed for DNA content to determine cell populations at 48 and 72 h after mock, rAd-vector and rAd-vpr infection. In the order of increasing DNA content, dead cells are shown in the sub-diploid peaks, G1 phase populations in diploid peaks, S phase cells in the plateau area and G_2/M cells in the polyploidy peaks

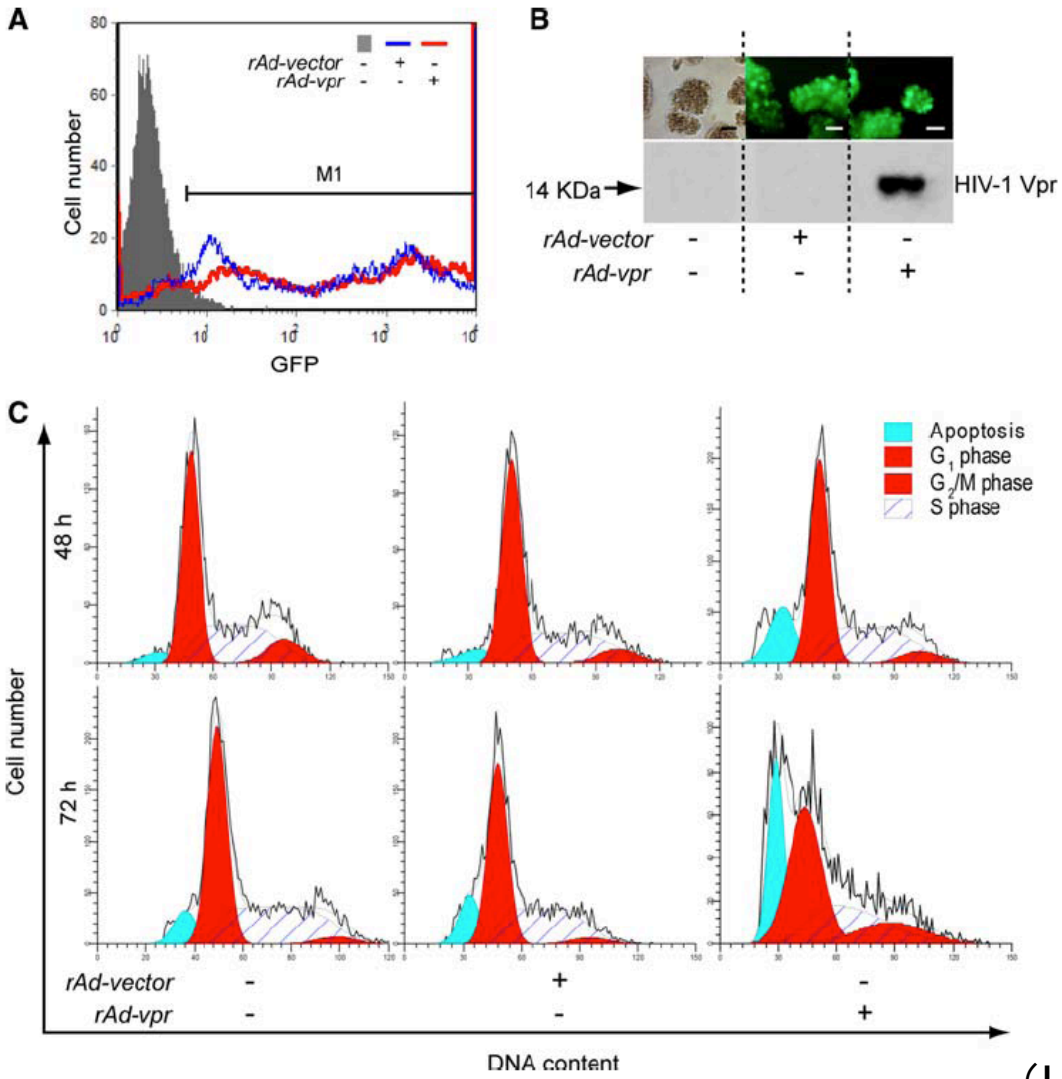

（He et al, 2009）

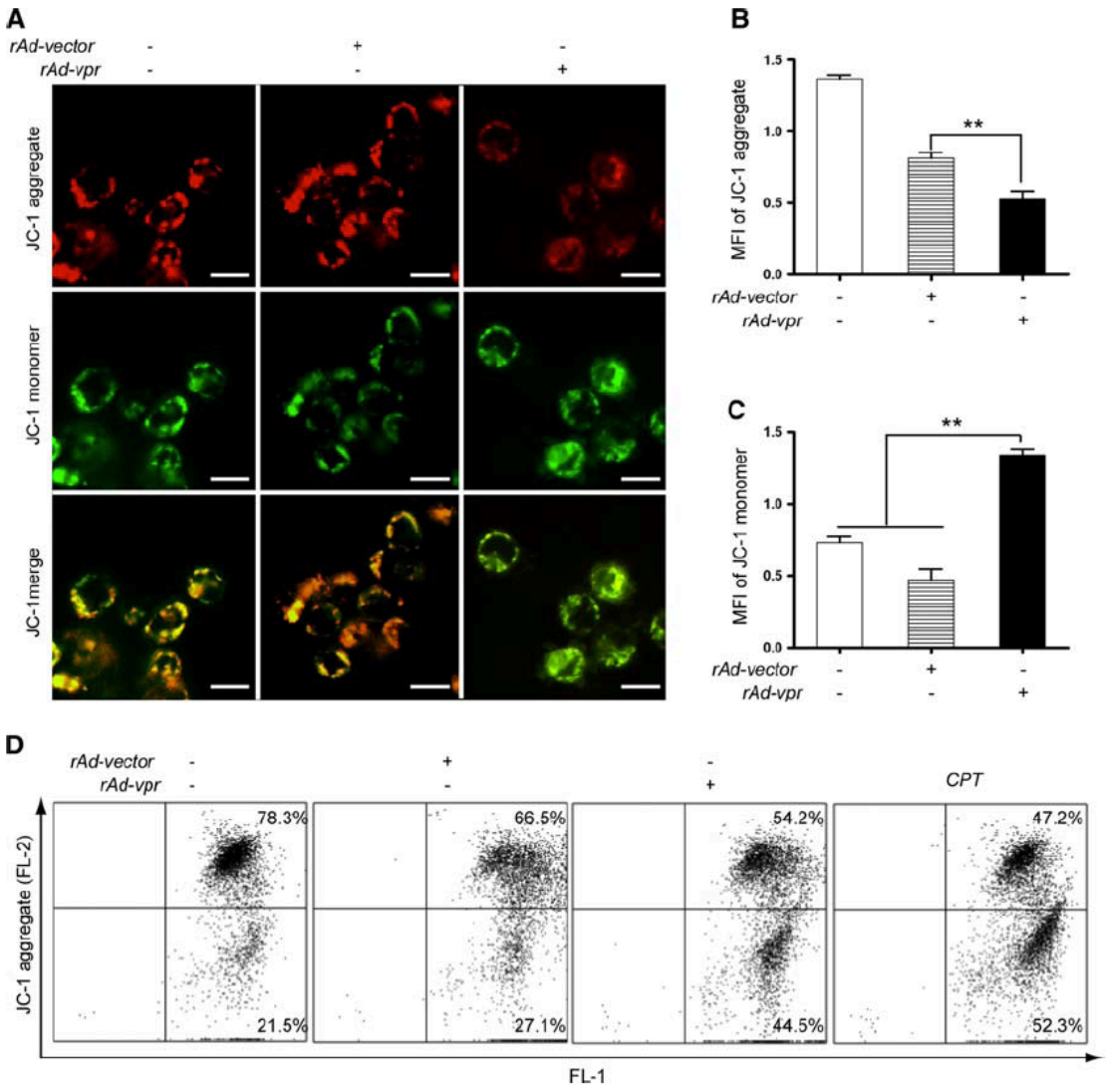

Fig. 2 Mitochondrial membrane potential loss was induced by endogenous Vpr expression in C8166 cells. Cells with mock- and viral infections as well as CPT (0.5 μmol/l) treatment were cultured for 24 h prior to JC-1 staining. **a** JC-1 aggregate and monomer observation. Images shown are representative observations from three independent experiments. Red images indicate the JC-1 aggregate fluorescence from healthy mitochondria, while green images exhibit cytosolic JC-1 monomers. Merged images indicated the co-localization of JC-1 aggregates and monomers. *Scale bar* = 10 μm. **b** MFI quantification of JC-1 aggregate in mock-, rAd-vector and rAd-*vpr* infected groups. **c** MFI quantification of JC-1 monomer in different groups. **d** MMP loss assay by FACS. Data are shown as mean ± SEM. One-way-ANOVA analysis, $n = 3$. ** $P < 0.01$

（He et al, 2009）

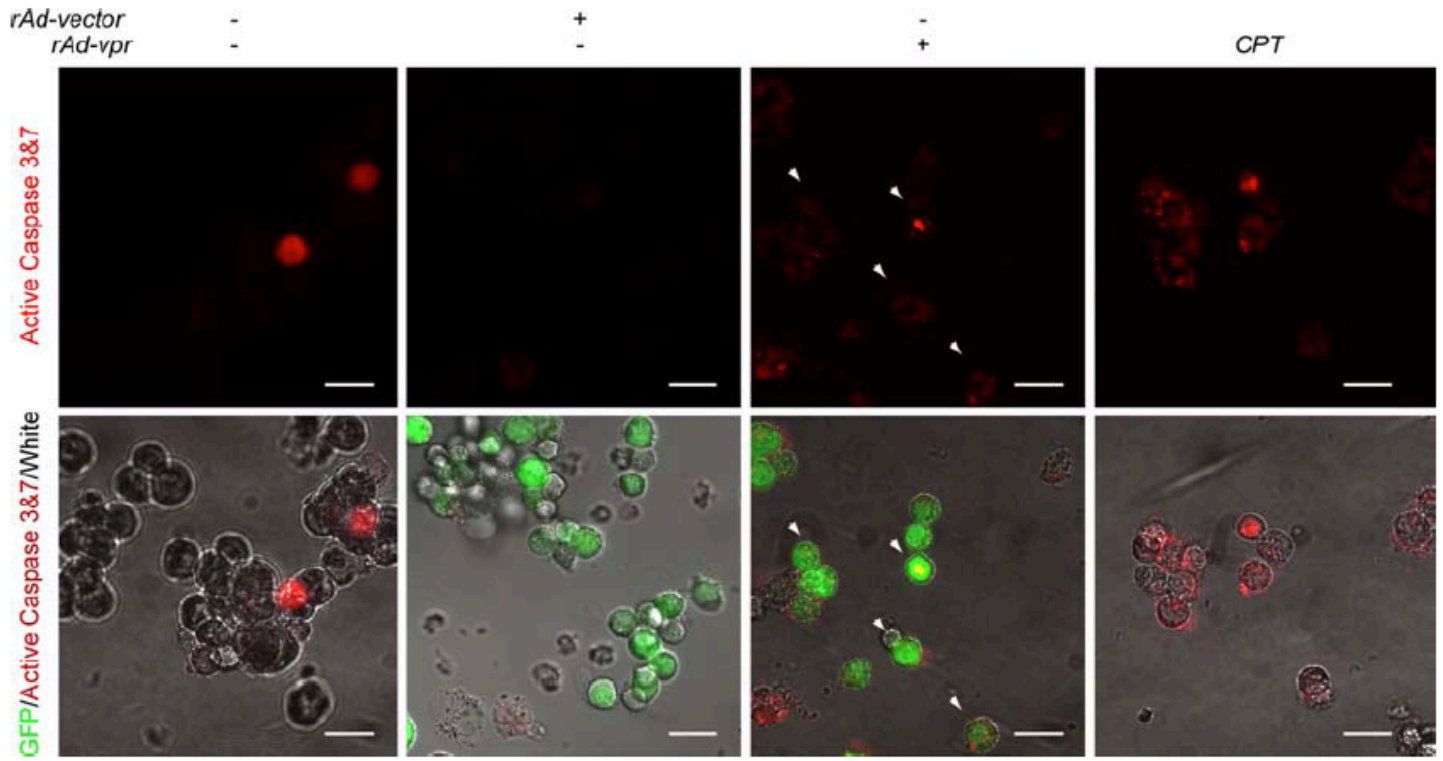

Fig. 5 Endogenously expressed Vpr induces up-regulation of caspase 3&7 activity in C8166 cells. Mock-, rAd-vector and rAd-*vpr* infected as well as CPT (0.5 μmol/l) treated cells were cultured for 24 h before being labeled by red FLICA. Images in the upper row show the active caspase 3&7 in the C8166 cells of different groups, while those in the lower row indicate the merged images of GFP, active caspases 3&7 and white field. *Scale bar* = 20 μm

（He et al, 2009）

Functional proteomic investigations on

Macrophage-HIV DNA-cancer cells

Acknowledgement

University of Washington

Charlotte Pan, B.S.

Sergei Ivanov, B.S.

Gregory Dann, B.S.

Jazel Dolores, B.S.

Dominic Forte

Zihuan Yang, PhD

Richard Fox, PhD

Thomas Andrus, MT

Jun Huang, MS

Tuofu Zhu, MD

NSFC

Grant number 81000516 (PI: T. Wang)

University of Nebraska

Howard Gendelman, MD

Pawel Ciborowski, Ph.D.

Jianuo Liu, M.D., Ph.D.

Nan Gong, MD

Irena Kadiu-Kiken, Ph.D.

Wojciech Rozek , Ph.D.

UW/FHCRC CFAR

New investigator award AI 27757 (PI: T. Wang)

Jinan University

The Fundamental Research Funds for the Central Universities of China, International (Grant number: 21610602) (PI: T. Wang)